Geomorphologic evidence for the late Pliocene onset of hyperaridity in the Atacama Desert

Ronald Amundson[1,†], William Dietrich[2], Dino Bellugi[2], Stephanie Ewing[3], Kunihiko Nishiizumi[4], Guillermo Chong[5], Justine Owen[1], Robert Finkel[2,6], Arjun Heimsath[7], Brian Stewart[8], and Marc Caffee[9]

[1]*Department of Environmental Science, Policy and Management, University of California, 130 Mulford Hall, Berkeley, California 94720, USA*

[2]*Department of Earth and Planetary Science, University of California, McCone Hall, Berkeley, California 94720, USA*

[3]*Department of Land Resources & Environmental Sciences, Montana State University, 817 Leon Johnson Hall, Bozeman, Montana 59717, USA*

[4]*Space Sciences Laboratory, University of California, Berkeley, California 94720, USA*

[5]*Departamento de Ciencias Geológicas, Universidad Católica del Norte, Antofagasta, Chile*

[6]*Center for Accelerator Mass Spectrometry, Lawrence Livermore National Laboratory, Livermore, California 94550, USA*

[7]*School of Earth and Space Exploration, Arizona State University, 548 Physical Sciences F-wing, Tempe, Arizona 85287, USA*

[8]*Department of Geology and Planetary Science, University of Pittsburgh, Pittsburgh, Pennsylvania 15260, USA*

[9]*Department of Physics, Purdue University, West Lafayette, Indiana 47907, USA*

ABSTRACT

The Atacama Desert has experienced a long and protracted period of hyperaridity that has resulted in what may be the most unusual biome on Earth, but the duration of this aridity is poorly constrained. We reconstructed aspects of the fluvial and geochemical history of this region using integrated landscape features (alluvial fans, hillslope soils, soil chemistry, river profiles) in the southern portion of the present desert. Topographic reconstructions of a large watershed (11,000 km^2) show deep incision and sediment removal between the late Miocene and the end of the Pliocene, and modest to negligible incision in post-Pliocene times. These changes in incision suggest an ~50–280× reduction in river discharge, which should reflect corresponding changes in precipitation. Changes in the nature of hillslope soils in the Atacama Desert indicate that in the Pliocene or earlier, hillslopes were mantled with silicate-derived soil. This mantle was stripped off and locally deposited as alluvial fans (late Pliocene to early Pleistocene) that now block or otherwise cause a rearrangement of Pliocene and earlier river channels. Finally, the hillslopes have largely accreted a soil mantle of dust and salt since the apparent late Pliocene stripping, suggesting a decline in annual precipitation of at least 125 mm yr^{-1} or more (mean annual precipitation [MAP] is now <3 mm yr^{-1}). Embedded in the long post-Pliocene era of salt accumulation, there are a variety of features suggesting overland flow on hillslopes (rills, striped gravel deposits, piping, and water spouts) and large, infrequent storms that infiltrated gentle alluvial fans (due to the depth of salt-rich horizons). Despite evidence for episodes that punctuate the hyperaridity, the magnitude and duration of these pluvial events have been insufficient to remove the regional accumulations of sulfate, chloride, and nitrate. The late Pliocene cessation of many fluvial features is coincident with recent research on the tropical Pacific, which shows that the Pacific was in a permanent El Niño state until ca. 2.2 Ma, at which time sea-surface temperatures offshore of South America declined greatly relative to those of the western Pacific, in turn setting up the present El Niño–Southern Oscillation (ENSO) climate system. These observations indicate that the latest period of aridity has been prolonged and largely continuous, and it appears to have occurred in step with the onset of the ENSO climate system, beginning ~2 m.y. ago.

INTRODUCTION

The Atacama Desert of northern Chile is among the driest places on Earth. When and why this region became so dry have long been a matter of debate. Regardless of the timing or mechanism for its aridity, the Atacama Desert is a truly unique environment. Due to very small and infrequent rains, much of the desert lacks higher life, and small populations of soil microbial life (Navarro-González et al., 2003; Maier et al., 2004; Warren-Rhodes et al., 2007) subsist on organic substrates that are believed to be largely atmospherically derived (Ewing et al., 2008a). As a consequence of this unusual climate, its long duration, and considerable regional volcanism, the region possesses the world's richest surficial accumulations of water-soluble anions such as nitrates, chlorides, bromides, borates, perchlorates, and iodates (Ericksen, 1981). The antiquity of this hyperaridity, and its origins, are topics that captured the attention of the earliest scientific explorers of the region (Darwin, 1845), yet definitive explanations for the onset of present conditions remain elusive, and most are highly debated.

While the Atacama Desert is unique relative to the rest of Earth, it lies within the southern Subtropical Convergence Zone belt, which includes the hyperarid desert of Namibia as well as the arid and semiarid regions of Australia (Houston, 2006). The atmospheric and oceanic circulation patterns that have conspired to make the Atacama a desert have also contributed to the general aridity of this latitudinal belt of the Southern Hemisphere. Thus, the climatic history of the Atacama Desert may ultimately be related to major changes in the global late Cenozoic climate.

The climate history of the Atacama Desert is important to several areas of research. First, the duration of aridity is needed to understand and model the region's unique chemistry and

†E-mail: earthy@berkeley.edu

GSA Bulletin; July/August 2012; v. 124; no. 7/8; p. 1048–1070; doi: 10.1130/B30445.1; 12 figures; 3 tables; Data Repository item 2012211.

biology (Navarro-Gonzalez et al., 2003; Rech et al., 2003; Michalski et al., 2004; Ewing et al., 2006, 2007, 2008a, 2008b). Second, it has been hypothesized that the onset of hyperaridity, and the resulting decrease in sedimentation in the offshore Peru-Chilean Deep Ocean Trench, is the cause for high rates of uplift of the northern Andes (Lamb and Davis, 2003). This hypothesis is not universally accepted, and the great height of the northern Andes has also been interpreted to be a result of the precipitation dependence of erosion rates in the Andes and the corresponding latitudinal changes in rainfall (Montgomery et al., 2001), although the correlation is complex (Bookhagen and Strecker, 2008). Third, well-constrained records are needed to understand the linkage of continental climate to marine circulation records (Ravelo et al., 2004). Finally, an understanding of the duration of the present climate structure will be a guide to considering the response of the region to anthropogenic climate forcing (Ravelo et al., 2006; Vecchi et al., 2006).

The climate record of the Atacama Desert is recorded in proxies of varying spatial and temporal clarity. Fossil rodent middens on the periphery of the largely plant-free desert proper provide relatively high-resolution perspectives of vegetation (and thus, precipitation) changes within the relatively short time frame of radiocarbon dating (Betancourt et al., 2000). On longer time scales, sedimentary evidence in basin deposits (Hartley and Chong, 2002) provides information on changes in sedimentary processes and basin hydrology that can be linked to changes in precipitation. The thickness and mineralogy of offshore sediments derived from continental erosion have suggested Quaternary oscillations in rainfall (Hebbeln et al., 2007). These records, while capable of providing important temporal information, record relatively recent events, unique geographical settings, or local conditions. Recently, paleosols embedded within continental sediments (Rech et al., 2006) have been used to provide a view of soil formation and leaching in the Miocene. Finally, dating of relict fluvial deposits provides information on the longevity and preservation of landforms, information suggestive of long-term hyperarid climates (Dunai et al., 2005). In summary, no one terrestrial paleoclimate proxy is without various deficiencies (as well as strengths), and multiple proxies, viewed in concert, are desirable to understand the region's climate history.

Here, we used integrated signals of regional pedogenic and geomorphic features to study the timing of decreases in water-driven processes such as stream incision and sediment removal, hillslope soil erosion, and soil chemical weathering, which all nearly ceased due to an apparent reduction in precipitation. The termination of any of these processes suggests an onset of dryness, and if these features all changed in unison, they should thus provide a strong indication of both the timing and magnitude of regional climate change. In that vein, the purpose of this paper is to (1) establish the long-term signature of precipitation in geomorphic and pedological features along a rainfall gradient in northern Chile, (2) use soil and geomorphic features in the hyperarid "centrum" to constrain the significance and age of changes in fluvial activity, (3) interpret the suggested timing and magnitude of this aridification in relation to recent marine records, and (4) examine the implications of our interpretations to other research and to the potential of climate change.

ATACAMA DESERT AND NORTHERN CHILE

Geography and Climate

The Atacama Desert extends from ~18°S in southern Peru to ~27°S in Chile (Fig. 1). From the southern boundary of the plantless or "absolute" desert, precipitation increases with increasing latitude (Fig. 2A). The extreme aridity of the region is due to four factors: (1) its position within the subtropical high-pressure belt caused by descending air from Hadley circulation; (2) the upwelling cold water immediately offshore, which reduces the moisture-holding capacity of air and creates a strong inversion layer that generally holds this moist air below 1000 m in elevation; (3) the presence of the Andes to the east, which block Atlantic-derived moisture; and (4) a regional circulation of rising air along the Altiplano and a corresponding subsiding return flow over the basins to the west (discussed in Houston, 2006; Rutllant et al., 2003). In addition to these factors, there is a pronounced change in seasonality, and source, of rainfall from south to north in Chile. In general, the frequency and abundance of westerly winter moisture decline with decreasing latitude, and the corresponding frequency and abundance of summer rainfall derived from easterlies overtopping the Andes increase. Between ~24°S and 18°S, coastal and low-elevation precipitation declines to levels of 3 mm yr^{-1} or less (Houston, 2006). In this study, we focused on the region between Antofagasta (23.45°S) and La Serena (29.90°S). Along this transect, there is a significant increase in precipitation from 3.5 mm yr^{-1} at Antofagasta (1939–1981) to 119 mm yr^{-1} at La Serena (1869–1989; www.worldclimate.com; Fig. 2A).

To a first order, the physical geography of this study area is characterized, from the coast to the east, by a narrow discontinuous belt of uplifted marine terraces, a discontinuous Coastal Cordillera, which reaches elevations up to 2000 m, and a broad inland lowland known as the Central Depression, which ranges from 1000 to 1500 m above sea level (asl; Figs. 3A and 3B). This region, which lies between the Coastal Cordillera and the pre-Andean Cordillera (Domeyko Range) to the east, varies both in width and in the abundance of local mountain ranges. The Domeyko Range, which reaches elevations of up to 5000 m asl, separates the Central Depression from a narrow, discontinuous pre-Andean depression that contains numerous internally drained salars. In general, the surficial expression of active tectonism increases greatly to the east of the Domeyko Range. To the east of the pre-Andean depression, the Andes proper rise to elevations exceeding 6000 m. This general topographic framework exists as far south as Vallenar (~28°S), at which point the Central Depression disappears as a distinct geographical feature, and series of mountain ranges, of increasing elevation, extend from the coast inland.

METHODS

To provide insights into the chronic impact of differing quantities of rainfall on an array of landscape features and processes in the hyperarid Atacama Desert, northern Chile is considered here as a multi-million-year rainfall experiment. With increasing southerly latitude, rainfall systematically increases, allowing us to decipher the integrated landform response to differences in precipitation. As we will discuss, this gradient reveals that surficial features in the most hyperarid segments are highly susceptible to even small increases in rainfall, and the existence of these features over millions of years is a testimonial to the long-term duration of climate conditions similar to those of today.

The geological information for the study was derived from maps produced by the Servicio Nacional de Geologia y Mineria of Chile. While the Coastal Range and the Central Depression contain a variety of rock types that record the geological evolution of the South American coast, Mesozoic granitic rocks (along with Mesozoic and Cenozoic volcanics) are abundant. In our work, we focused on hillslopes, terraces, and the fluvial deposits derived from these features. The maps are available at various scales, and vintages, and are partially available in digital formats. For maps critical to our study area that were not in a digital format, the printed maps were digitized by GEOVECT, Austin, Texas. For maps used in landscape evolution reconstructions (discussed herein), field checking was conducted to verify, and in a few cases reclassify, key map unit assignments.

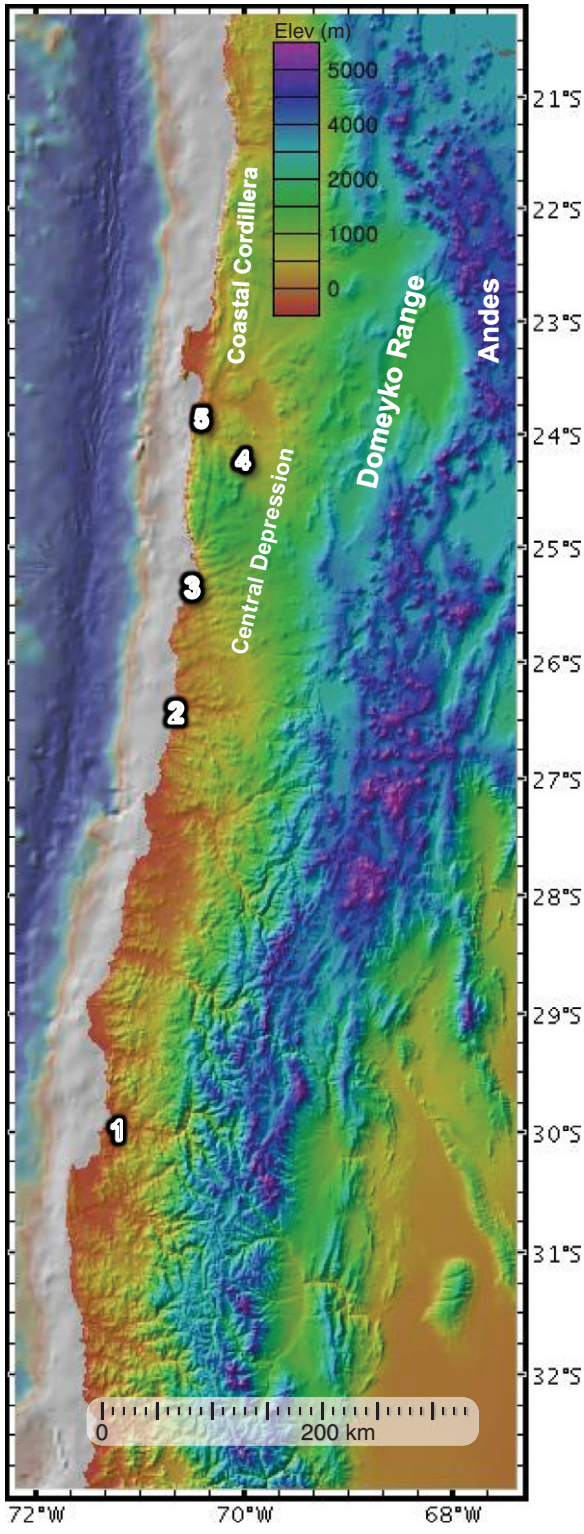

Figure 1. Colored shaded relief digital elevation model (DEM) of northern Chile, and the location of key field areas. 1—La Serena, 2—Chanaral, 3—Taltal, 4—Aguas Blancas, 5—Antofagasta.

Landscape reconstructions of basin fill from the Miocene to the present were obtained by overlaying the digital geological maps on the Shuttle Radar Topography Mission (SRTM) topographic data for the region. Paleosurfaces were reconstructed by classifying the SRTM data into Miocene, Pliocene, and modern fluvial features. Elevations were determined by interpolating between paleosurfaces using TOPOGRID, an iterative finite-difference interpolation technique designed to create hydrologically correct digital elevation models (DEMs). Based on Hutchinson (1989), it is essentially a discretized thin-plate spline technique, such as that used by Wahba (1990), where the roughness penalty has been modified to allow the fitted DEM to follow abrupt changes in terrain (such as streams and ridges), and with an adaptive root mean square (RMS) interpolation error (Hutchinson, 1996). For the Miocene surface reconstruction, the SRTM data were limited to the areas mapped as Miocene-dated geologic units. For the Miocene to Pliocene erosion estimates, the SRTM data for Pliocene geological units were interpolated to create a Pliocene surface that was then subtracted from the previously constructed Miocene surface. A similar procedure was used for the Pliocene to Quaternary erosion value. In all basin infill reconstructions, topography that rises above the basin infill was excluded from erosion calculations. To compute erosion between the different eras (Miocene, Pliocene, and modern), the corresponding DEMs were subtracted, and the resulting elevation differences were multiplied by the square of the grid cell size and then summed. The resulting volumes were divided by the time between the eras to obtain a rate.

Landform ages were derived from (1) geological maps, (2) published K-Ar dating of ashes within the region, and (3) cosmogenic radionuclide exposure ages of granitic boulders and quartz cobbles collected during this work. Approximately 500 g samples of rock were ground, and quartz grains were isolated through a series of acid treatments (Kohl and Nishiizumi, 1992). The ^{10}Be and ^{26}Al isotopes were isolated and purified using anion and cation exchange columns. Accelerator mass spectrometer (AMS) measurements of ^{10}Be and ^{26}Al were performed at the Lawrence Livermore National Laboratory AMS facility or at the PRIME Laboratory at Purdue University. We used half-lives of 1.36 m.y. for ^{10}Be and 0.705 m.y. for ^{26}Al (Nishiizumi, 2003; Nishiizumi et al., 2007). We used a ^{10}Be production rate of 5.1 atom yr^{-1} g^{-1} for ^{10}Be and 34.1 atom yr^{-1} g^{-1} for ^{26}Al (both in quartz), and a 1.5% muon contribution. The results were converted to minimum exposure ages and maximum erosion rates using the production rate scaling factors of Lal (1991) and site-specific location data. We adopted a mean attenuation length of 165 g cm^{-2} and a density of 2.70 g cm^{-3}.

The primary field area in the hyperarid zone was the watershed that drains toward the Pacific Ocean through the Coastal Cordillera via the Quebrada La Negra (Fig. 3A). The total area of the drainage is ~11,160 km^2, and, most importantly for this work, all surficial water is locally derived—streams do not transport surface waters from the Andes. The watershed is

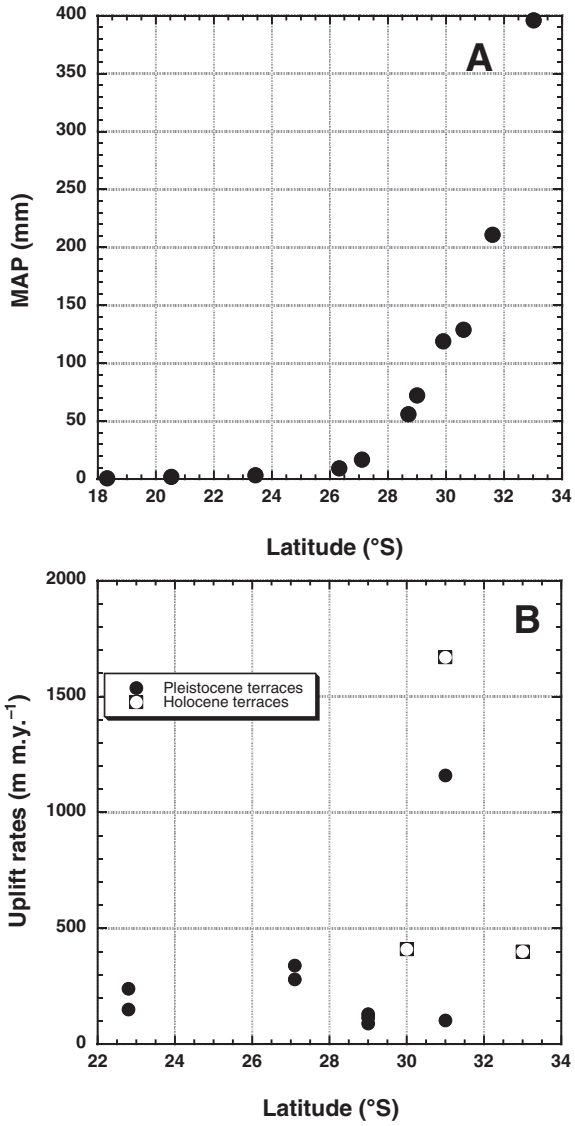

Figure 2. (A) Rainfall (mean annual precipitation [MAP]) versus latitude for coastal cities within our study area (http://www.worldclimate.com/) and (B) coastal uplift rates of Pleistocene and Holocene marines terraces (Saillard et al., 2007, 2009; Ota et al., 1995; Ortlieb et al., 1996; Leonard and Wehmiller, 1992; Marquardt et al., 2004; Quezada et al., 2007; Le Roux et al., 2005).

representative of the hyperarid region of the Atacama, and numerous studies have examined the geochemistry (Rech et al., 2003; Ewing et al., 2006, 2007, 2008a, 2008b), geomorphology (Owen et al., 2010), and biology (Navarro-González et al., 2003; Warren-Rhodes et al., 2007) in portions of this watershed.

Starting with this hyperarid reference region, we extended our observations as far south as La Serena (Fig. 1; Table 1). With increasing southerly latitude, rainfall increases by several orders of magnitude, and temperatures decline slightly (Table 1). Most importantly, ecosystems change from an absolute desert in the north to a coastal shrub community to the south. Sites along this transect have been used to examine the way in which soil chemistry (Ewing et al., 2006), the soil N cycle (Ewing et al., 2007), and hillslope processes (Owen et al., 2010; Dietrich and Taylor Perron, 2006) vary with increasing rainfall. Uplift rates along the transect (Fig. 2B) were taken from a variety of reports of ages and heights of marine terraces. Since most of the terraces are less than 500 k.y. old, the uplift rates are not necessarily indicative of longer-term tectonic uplift rates.

Soil observations were made in hand-dug exposures or on abandoned mining excavations. Some of the observations versus rainfall have been reported previously (Ewing et al., 2006). Vertical differentiation of soil horizons, and their field-observable characteristics, were made using standardized methods (Soil Survey Manual, 1993). Chemical analysis methods were described previously (Ewing et al., 2006).

To explore the qualitative way in which river profiles may respond to decreases in incision rates driven by declines in rainfall, the long profiles of streams crossing the Coastal Cordillera were constructed from Antofagasta to a southern reference channel. The long profiles were derived from the digitizer tools within GeoMapApp (v. 1.7.6). GeoMapApp is a Web-based access to global SRTM topographic data that also provides various display and analysis functions. At a latitude of ~29.4°S, the Coastal Cordillera disappears as a distinct geographic unit, and thus this was the southern termination of the comparison.

We hypothesized that the shape of the long profiles was as follows. Stream profiles at steady state form convex-up profiles based on steady-state solutions to analytical models incorporating the stream power erosion law:

$$E = KX^{\mathrm{mh}}S^{\mathrm{n}}, \quad (1)$$

where K is a dimensionless coefficient of erosion, and m and n are positive constants with values of 04–0.6 and ~1, respectively, and h is a constant ~1.6. X is the length of the channel. K reflects the climatic (rainfall) sensitivity of this incision model, as well as bedrock resistance and sediment supply effects. For an actively uplifting channel:

$$\frac{dz}{dt} = U - \left(KX^{mh}S^{n}\right). \quad (2)$$

where U = uplift rate. At steady state ($dz/dt = 0$), a concave stream profile is generated by this model (Whipple and Tucker, 1999). The solution of the steady-state version of Equation 2 is:

$$z = z_o + \frac{n\left(U/K\right)^{1/n}}{n - hm}\left(X^{1-\frac{hm}{n}} - X_o^{1-\frac{hm}{n}}\right), \quad (3)$$

where z_o and X_o are the elevation and distance from the summit, respectively, at sea level.

Since convex-up profiles represent non-steady-state conditions, we hypothesized that steady increases in upward convexity with decreasing latitude are due to a progressive decline in the value of the processes captured in K, although, alternatively, variations in uplift rate with latitude could also contribute to this trend. To test this hypothesis, we examined one of the main channels that drains an ~12,000 km^2 watershed near Antofagasta, a distinctively convex-up profile. Topography and hydrology data were obtained from http://hydrosheds.cr.usgs.gov/. The channel was selected from the HydroSHEDS coverage and overlaid onto the topography to obtain an elevation profile (Fig. 4). The length of this profile is 154,200 m, with a maximum elevation of 2148 m. Faults crossing this profile were manually digitized using the SRTM data at distances of 83,950 m and 143,300 m from the channel. The profile was

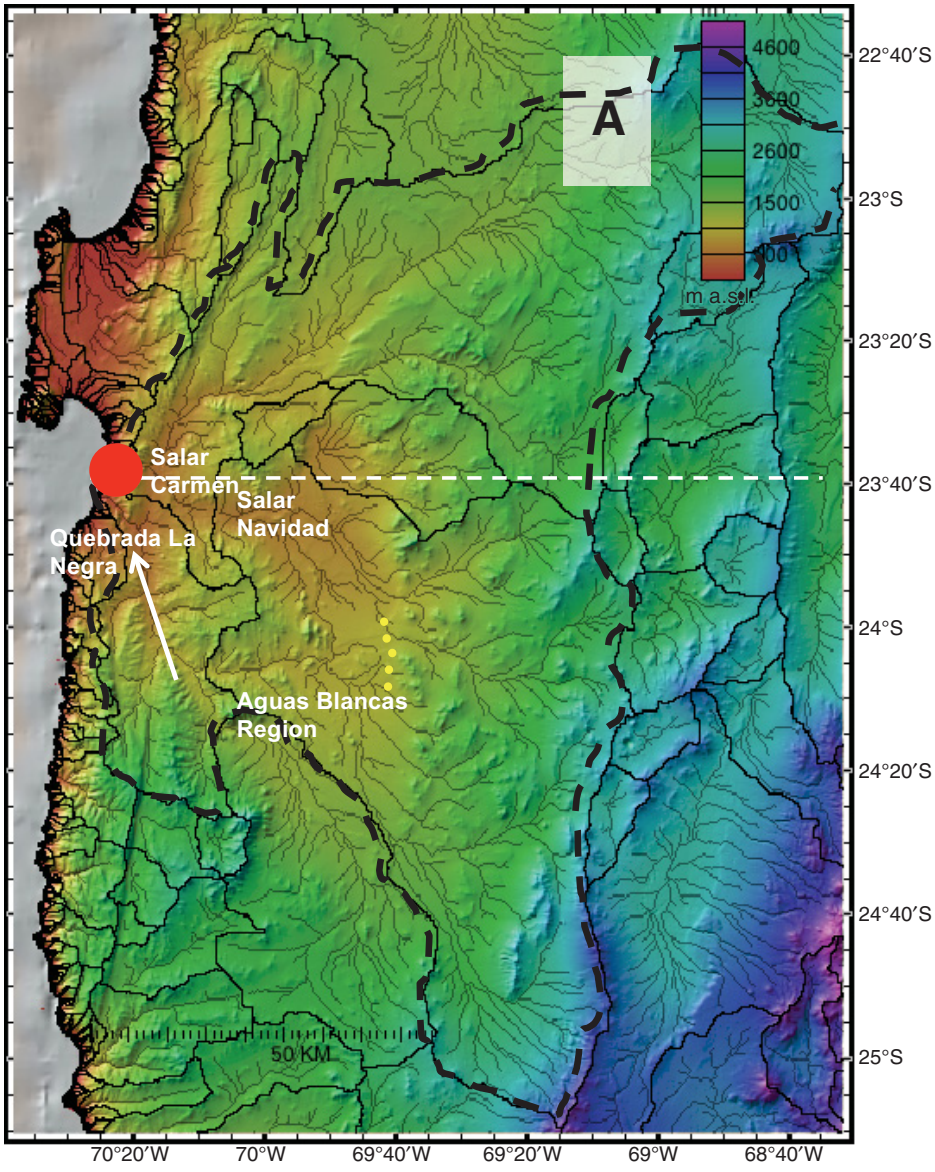

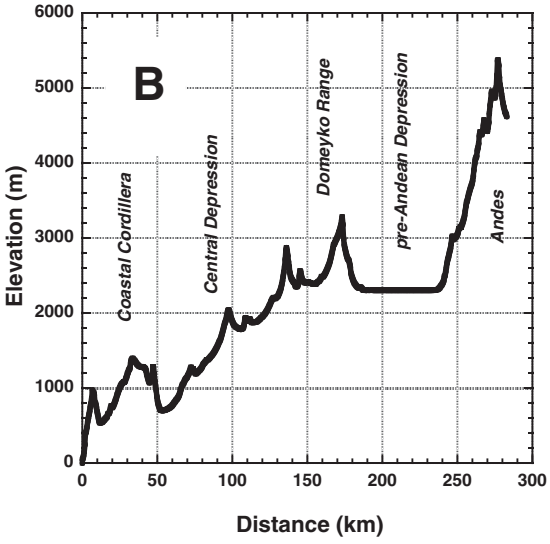

Figure 3. (A) Shaded relief digital elevation model (DEM) of the watershed that drains toward Antofagasta (red circle). White dashed line represents cross section illustrated in B. The outline of the watershed is indicated by the black dashed line. The point at which the present watershed drainage coalesces and enters the canyon of the Quebrada La Negra through the Coastal Cordillera is indicated by the white arrow. The red dotted line shows a prominent trace of the Atacama fault, and the yellow shows the Falla Boquete. (B) A topographic cross section from Antofagasta to the Andes illustrating the key geographical features of the region.

then resampled at 50 m intervals, and smoothed using a moving-window Gaussian filter. An analytical profile was generated based on Equation 3, the parameters used were:

U = 100/1,000,000 (uplift rate, m/yr),
M = 0.5 (area exponent),
N = 1 (slope exponent), and
H = 1.67 (area-length exponent).

K was allowed to vary in order to match the real profile's height, resulting in a value of 1.75145 × 10^{-6} (erosion coefficient, $m^{[1-2M]}$/yr). To place the start of the resulting profile at sea level, Z_0 was set to 10 m.

A numerical model was developed that represents Equation 2. An initial U vector and final U vector, as well as initial and final K vectors, were used to obtain the appropriate U and K values by linear interpolation. K varied uniformly over the entire profile, while U represented different regimes. These regimes represent different regional tectonics (source to fault 1, fault 1 to fault 2, fault 2 to ocean). Three different experiments were performed with the numerical model to determine whether the present-day long non-steady-state profile could be caused by reductions in K, increases in U, or some combination. The results of the experiments are discussed next.

RESULTS AND DISCUSSION

Soil and Geomorphic Features versus Rainfall in Modern Chile

We first examine the ways in which pedological and geomorphological processes in modern Chile respond to precipitation. Key diagnostic characteristics of the changing climate zones are soil chemistry and hillslope processes. Near La Serena, hillslopes are mantled with silicate-rich soil material derived from the underlying rock (Figs. 5A and 5B). Soil production and sediment transport are largely biologically mediated by burrowing animals, insects, and plants. Hillslope and alluvial fan/terrace soils are salt (carbonate) free, exhibit reddish brown colors, and, on stable surfaces, have distinct clay-rich horizons from chemical weathering and possibly eolian inputs. Based on hillslope bedrock erosion rates (Table 1), soil characteristics, and vegetation, the area is similar to semiarid regions in Australia (Heimsath et al., 2001) and California (Heimsath et al., 1999). At ~29.25°S between La Serena and Vallenar, increasing aridity causes the retention of carbonate in both hillslope and level surfaces. Vegetation cover declines, but soil production and transport are still largely biotically driven. With decreasing

TABLE 1. CLIMATE DATA AND AVAILABLE HILLSLOPE EROSION RATES ALONG THE CLIMATE GRADIENT EXAMINED IN THIS STUDY

Site	Latitude (°S)	Longitude (°W)	MAP (mm)	MAT (°C)	Erosion rate (m m.y.$^{-1}$)*	Plant cover (%)
La Serena	29.9	71.2	119	13.6	~25	32
Vallenar	28.6	70.7	56.1	15.3	nd†	nd
Chanaral	26.32	70.59	9.5	~16	~2	6
Antofagasta	23.43	70.4	3.5	16.4	~<1	0

Note: MAP—mean annual precipitation; MAT—mean annual temperature.
*Owen et al. (2010).
†Not determined.

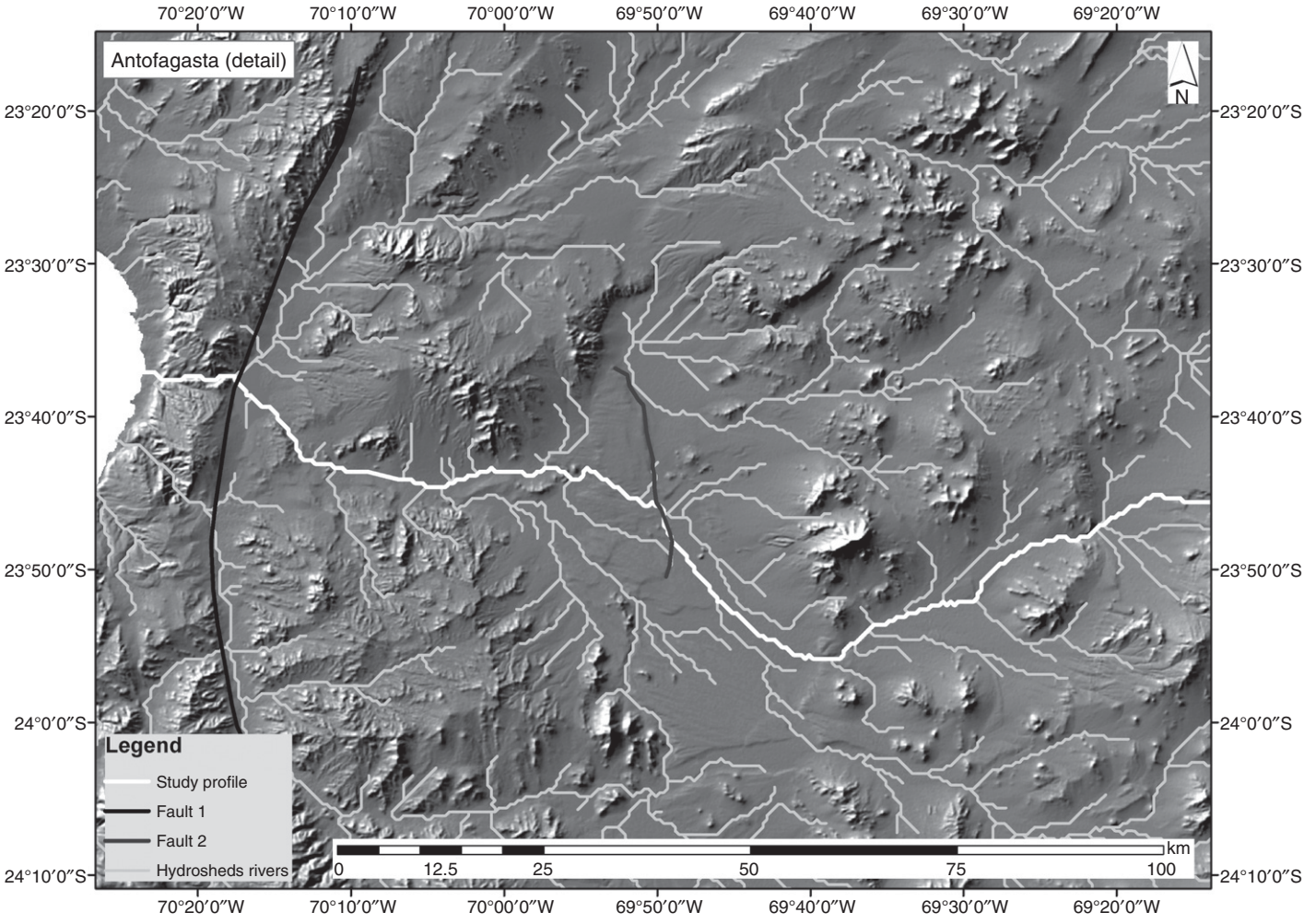

Figure 4. A digital elevation model (DEM) of the Quebrada la Negra watershed, with channel patterns, as determined by the Hydrosheds model. The most prominent light-toned line is the channel used for the long profile analysis discussed in the text.

latitude and rainfall, vegetation thins, and the soil cover becomes both thinner and patchier, resulting in a broad region between roughly 27°S and 26.25°S where hillslope soil cover is absent or only a few centimeters thick, sediment transport appears to be due mainly to overland flow, and erosion rates are an order of magnitude lower than at La Serena (Table 1; Figs. 5C and 5D). Carbonates are commonly absent in the soils (except immediately adjacent to sparse plant roots), and Ca sulfates are present in the thin soils on the hillslopes, and in the much thicker soils on alluvial fans. On the hillslopes, there is a sharp transition between the very thin soil cover and the fractured, chemically fresh bedrock (Fig. 5D). A thin soil-bedrock transition zone of a few centimeters is common. Water- and/or salt-driven processes corrode the upper rock contact, slowly spalling off grains and small fragments that become part of the active soil layer. This layer is removed from the landscape at rates comparable to or faster than the rate it is produced. Close inspection of fractured rock at the base of the soil also revealed fine-scale plants and root hairs, so biotic processes may play some role in breakdown.

Further to the north, the decline in rainfall results in large changes in the nature of the landscape (Figs. 5E and 5F). The landscape lacks plants, and soils on both hillslopes and on level geomorphic surfaces contain large quantities of sulfates, chlorides, and nitrates. Rates of hillslope bedrock erosion or soil production are

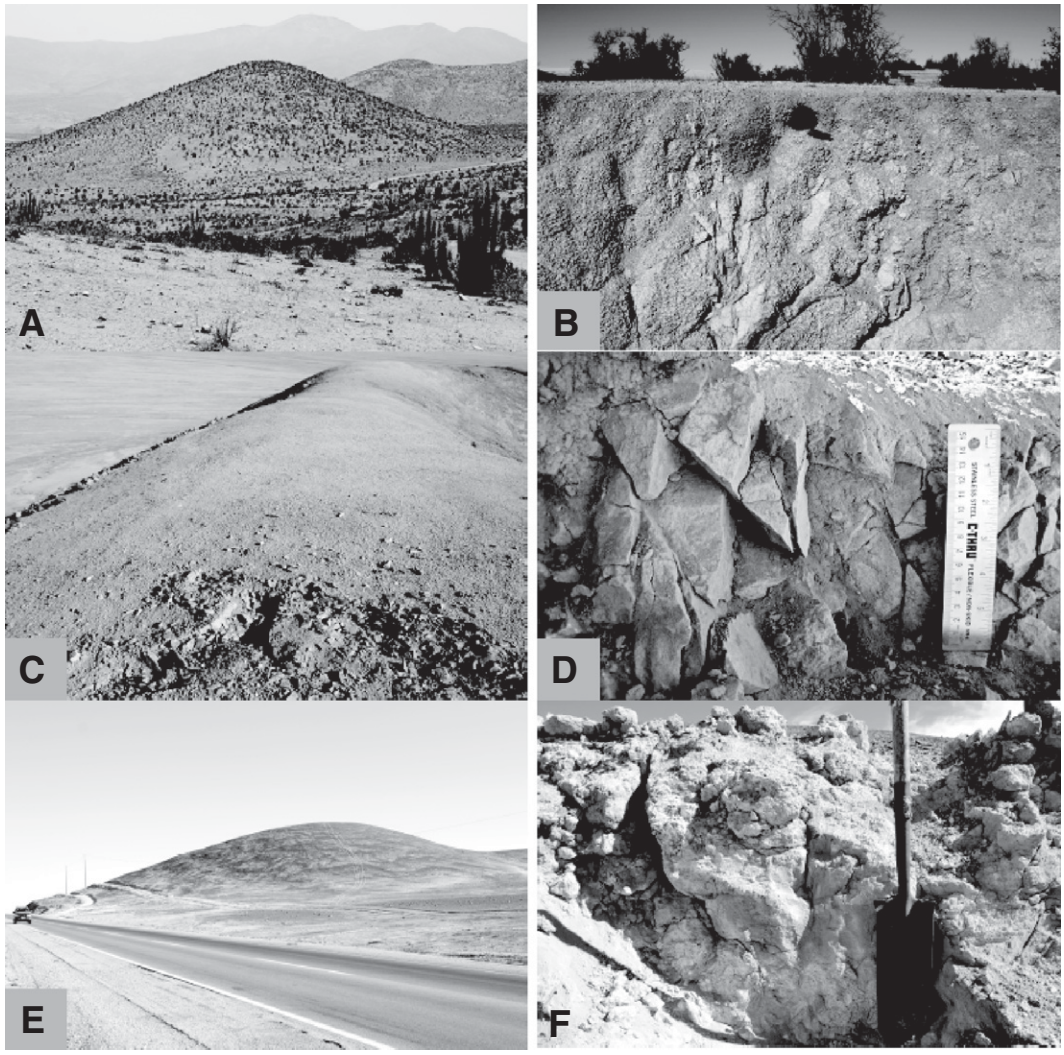

Figure 5. (A) A typical vegetated, soil-mantled hillslope near La Serena, (B) bedrock-derived soil cover over saprolized bedrock near La Serena, (C) gently convex, nearly soil-free (note bedrock exposure near forefront) hillslope north of Chanaral, (D) thin (cm) mobile soil layer over fractured, but chemically unaltered bedrock, in area of C, (E) salt/dust-mantled hillslope immediately SW of Aguas Blancas, and (F) thick (50 cm+) sulfate-rich soil showing large subvertical cracking associated with hydration/dehydration processes.

almost another order of magnitude lower than that of the next wetter site. Soil production from bedrock erosion appears to be achieved by salt-mediated physical processes such as shrinking and swelling (see resulting cracks in Fig. 5F). Sediment transport off hillslopes appears to be due to a combination of physical shrink-swell of sulfate salts and overland flow during rare rainfall events. The bedrock (and rock fragments in the soil) is entirely free of chemical weathering and has experienced only physical fracturing by salt.

These observations indicate that distinctive rates and types of landscape processes (and resulting properties) occur along this modern rainfall gradient. The processes and characteristics of the semiarid environment are similar to many others around the world: hillslope processes that are biologically mediated, soils exhibiting chemical weathering of silicate parent materials, and a lack of salts (even carbonate) due to insufficient precipitation. In geomorphic terms, the hillslopes there are transport-limited. The intermediate zone (arid-hyperarid boundary) is at the rainfall limit of life (and many plants there appear to subsist mainly on fog water). Plant cover, to stabilize soil, is nearly absent, while production rates from the underlying rock (largely chemically driven) set the erosion rate. This is a weathering-limited landscape. The northern end member is unique on Earth. Atmospherically derived soil (dust and salts) mantle most of the landscape (except in the few active channels that exist on the landscape). Because sediment transport processes are so hindered by lack of life and water, the landscape is transport limited, with much of the soil production is derived from atmospheric deposition as opposed to bedrock weathering (Owen et al., 2010).

Changes in precipitation result in large and systematic changes in soil production rates. These changes are also reflected in the incision rates of major streams bounding the hillslopes, those that are parts of drainages that traverse the Coastal Cordillera and drain the large, interior basins. Coastal uplift occurs along much of the northern Chilean coast, leaving evidence in the form of marine terraces (e.g., Quezada et al., 2007; Saillard et al., 2007). Figure 2B illustrates that there is no discernible trend in uplift rates versus latitude, although there is considerable variation. A recent uplift compilation by Rehak et al. (2010) showed that uplift rates increase at ~33°S, south of the focus of our work. Mortimer (1980) first showed that there are distinct changes in stream profiles from convex downward to convex upward, from south to north, respectively, reflecting the decreasing abilities of streams to maintain grade with uplift as mean annual rainfall declines. A similar trend was observed by Montgomery et al. (2001), who focused on the shapes of the general landscape on the west side of the Andes. Next, we will examine in more detail the possibility that this channel trend reflects post-Miocene changes in stream capacity.

Evidence of Climate Change

Rates of Watershed Erosion

The watershed of the Quebrada La Negra is a large system confined to the Central Depression proper (Fig. 3A). The upper reach of the watershed, in the Cordillera Domeyko, achieves elevations exceeding 4000 m. Despite these high elevations, the watershed remains hyperarid, is free or nearly free of plants, and possesses soils containing sulfates and other salts over its entire extent. Most runoff infiltrates into the sediments during transport, or evaporates in one of several playas, rather than exiting to the Pacific. As will be discussed, this largely internal drainage appears to be a post-Pliocene phenomenon. The southern half of the watershed (where most of our observations have been made) drains to the north and enters a series of playas near Aguas Blancas, an important salt-mining region (Figs. 3A and 6A). A narrow overflow outlet to the north drains the playa and eventually terminates in the internally drained Salar de Navidad (Figs. 3A and 6C). Thus, in combination with internal drainage in the Salar de Carmen, much of this large watershed is now internally drained, and only a small fraction of the watershed is topographically capable of supplying surface runoff to the Quebrada La Negra, and the Pacific Ocean. South of Aguas Blancas, present stream drainages are incised a few meters or less into older sediment and, in many locations, flow on top of older deposits (as originally noted by Mortimer, 1973, 1980). These observations show that the present drainage system, despite its size and elevational diversity, is discontinuous, and little water and sediment make it to the Pacific Ocean. While the present drainage system is characterized by hydrological ineffectiveness, the older fluvial features suggest vigorous periods of regional deposition and erosion.

The Quebrada La Negra (Fig. 3A) has maintained an active stream profile as coastal uplift has occurred. The presence of Miocene river gravels where the river crosses the coast range suggests it has been active since at least that time. In addition to uplift, the coast of this portion of Chile is hypothesized to be undergoing a subduction-driven landward erosion of the coastline of up to 1 km m.y.$^{-1}$ (von Huene et al., 1999), which also impacts base level for the stream. A second stream located a few kilometer to the north, the Quebrada Caracoles, also crosses the Costal Cordillera, reaching the sea in northern Antofagasta. However, the Quebrada Caracoles is currently hydrologically isolated from the Central Depression by accumulations of locally derived sediment that block the upper section of the canyon (creating a drainage divide) near its junction with the Central Depression. González et al. (2006) obtained an exposure age of 400–500 ka on offset alluvial fans using cosmogenic ^{21}Ne. The offsets are up to 9 m. We measured cosmogenic radionuclide exposure ages of 276 and 336 k.y. on amalgamated gravel samples (samples CRC-06–1 and CRC-06–2; Table 2) from an alluvial fan that accumulated near the valley-fault margin. Because the fan represents the depositional response to the cessation of flow through the canyon, its younger age is consistent with the independent assessment for timing of fault offset. Sediment and water now accumulate in the Salar del Carmen Depression, which lies just to the east of the Atacama fault.

In the following sections, the history of alluvial deposition and dissection in this drainage basin is reconstructed from the Miocene to the present. By reconstructing the landscape at different key points in time (as indicated by the remaining geomorphic surfaces), we can develop an understanding of the large changes in rates of fluvial processes that have occurred since the late Miocene, and pinpoint those consistent with the onset of nearly continuous hyperaridity.

Miocene deposition and erosion. Here, we focus on the erosional and depositional history of the basin sediments of the Central Depression, ignoring contributions from bedrock that outcrops in numerous hills and small mountain ranges. The bedrock, a diverse mix of metasedimentary and volcanic rocks of Paleozoic to Cenozoic age, currently erodes at a rate of ~1 m m.y.$^{-1}$ (discussed earlier), and we therefore assume that the bedrock topography has remained relatively constant over the time interval of interest here.

The surficially exposed sedimentary deposits are of Tertiary and Quaternary ages, and are largely mapped as three units: Oligocene–Miocene, Pliocene,[1] and Quaternary. To allow the reader to visualize the geology and the age constraints in detail, we provide a kmz file (viewable in Google Earth), as well as a jpg file, of the general geology with the dates in Table 2 overlain on the general geological map of Chile (GSA Data Repository Figs. DR1 and DR2).[2]

The highest standing alluvial landforms are broad plains or mesas consisting of an Oligocene to Miocene accumulation of gravel and sand, with occasional interbedded ignimbrites. In the southern part of the watershed, they are mapped as the Formacion Pampa de Mulas (Marinovic et al., 1992). Other more recent maps refer to these gravels as Mg (lower to mid-Miocene deposits).

Observations of LANDSAT imagery, field observations (Fig. 7), and DEMs reveal that these deposits are modestly faulted and deeply incised along major drainages, or buried by younger deposits along mountain fronts. These Tertiary gravels have the steepest gradient of the fluvial features in this region (~12 m/km vs. ~7–8 m/km for Pliocene channels in the vicinity of Aguas Blancas). Topographic profiles of these deposits in the vicinity of Aguas Blancas (presently a local base level) show drainage trajectories through canyons to the west and east of Cerro de Los Tetas (label on Fig. 6). These canyons now contain drainage divides blocked by alluvial fans from local drainages (Fig. 6A). Field observations along highway B-55, ~10–20 km east of PanAm 5 highway (Fig. 8), reveal the presence of at least two strath terraces and a stream-beveled mid-canyon ridge that (1) are at the same height projected by Miocene infilling (discussed later herein) and (2) drain downslope toward Antofagasta. The slope of the straths is ~13 m/km, consistent with the slope of the Miocene alluvial surface immediately upslope. The height and slope of the remnant bedrock terraces are supportive of Miocene stream activity and sediment transport toward the Quebrada La Negra and the Pacific Ocean. However, the valley is now blocked by local sediment that forms a drainage divide (Figs. 6B and 8).

All these Tertiary deposits are commonly known as the "Atacama Gravels," Miocene alluvial fills and pediments, identified as far south as La Serena (latitude 30°S) by Mortimer and others (e.g., Mortimer, 1973, 1980). The relative thickness of the gravels, approximately tens of meters to ~100 m depending on location (Riquelme et al., 2007), combined with ages of intercalated ashes and ignimbrites, indicates that deposition of these gravels occurred over an extended period of several million years (e.g., Clark et al., 1967; Riquelme et al., 2007). Recent work by Riquelme et al. (2007) and Nalpas et al. (2008) along the Rio Salado (near Chanaral, Fig. 1), to the south of our primary study area, suggests that the infilling of the Central Depression began with the burial of an Oligocene erosional landscape formed during a more pluvial period, and continued during a long period of declining precipitation. Nalpas et al. (2008) concluded that deposition ceased with the onset of hyperarid conditions, between

[1]The recent change in the Pliocene-Pleistocene boundary (Gibbard et al., 2009) from 1.8 to 2.6 Ma may ultimately change of some the epoch assignments of the geological mapping units in our field area. In our landscape reconstructions, we use the previously assigned relative geological ages, where the Pleistocene was assigned a beginning at 1.8 Ma.

[2]GSA Data Repository item 2012211, Figure DR1 is a geological map of the watershed examined with both new and published geochronological age controls based on cosmogenic exposure ages or K-Ar dating of volcanic ash. Figure DR2 is a kmz version of Fig. DR1 suitable for viewing in Google Earth, is available at http://www.geosociety.org/pubs/ft2012.htm or by request to editing@geosociety.org.

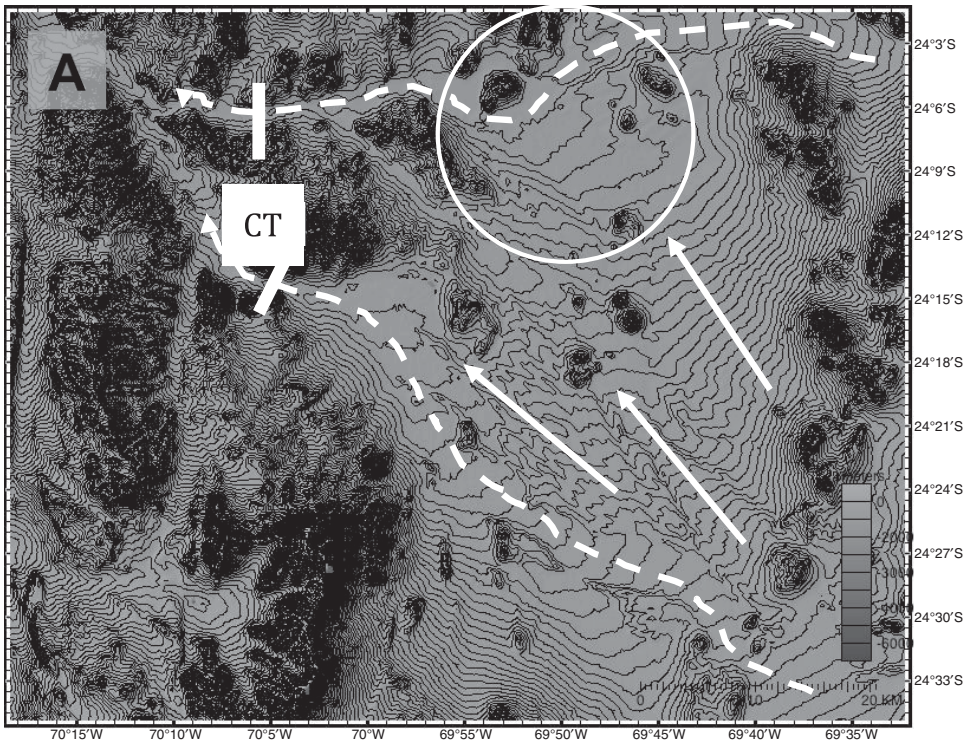

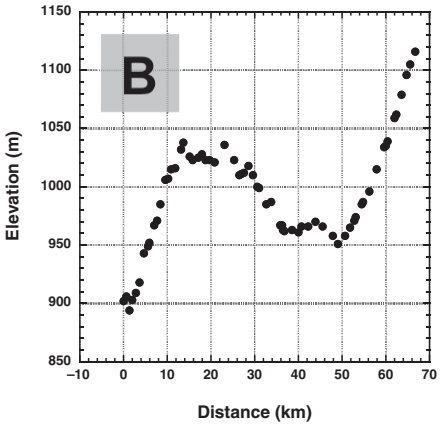

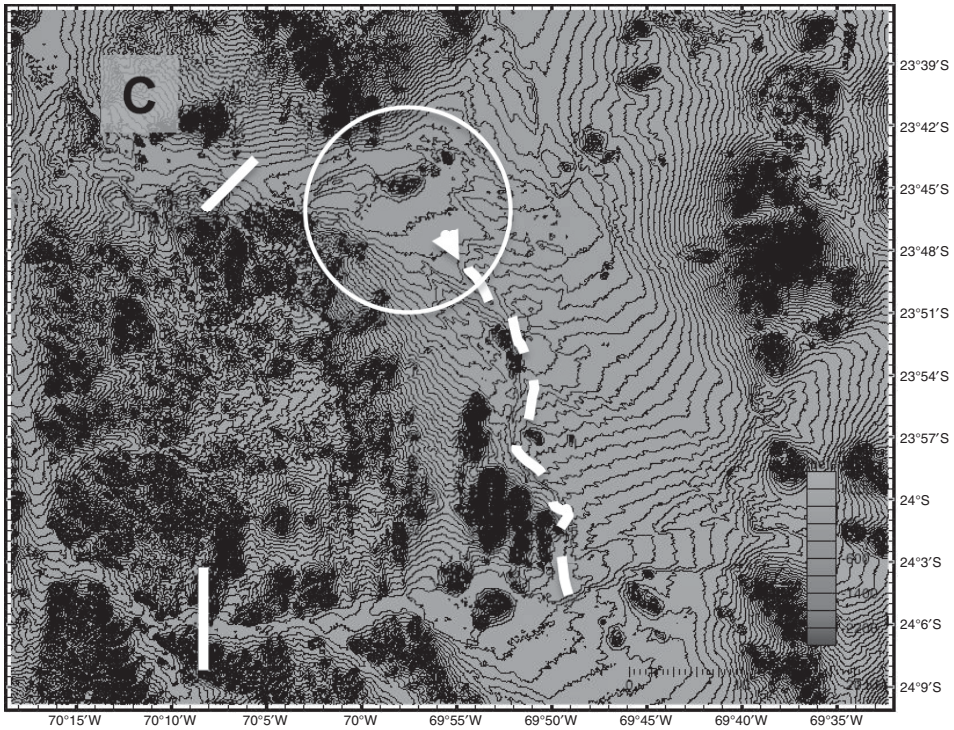

Figure 6. (A) A digital elevation model (DEM) (10 m contour intervals) of the Aguas Blancas salar (playa) (white circle). White solid arrows show the location and general slope of Miocene fans and fan remnants. White dashed lines reveal location and direction of Pliocene channels inset into the Miocene features. The box labeled CT refers to the location of the Cerro de la Tetas. (B) A topographic profile of the canyon/channel shown by the dashed line near the top of A. The profile reveals significant infilling of the canyon downstream of the channel, with a local drainage divide caused by small fan infilling from ranges on both sides of the canyon. The locations of alluvium-derived drainage divides are illustrated by white solid lines perpendicular to projected Pliocene stream flow. (C) A DEM (10 m contour intervals) showing the region directly north of Aguas Blancas. Dashed line reveals the location and direction of post-Pliocene stream capture. White circle identifies the general location of the Salar de Navidad, the local base level for the drainage. Local drainage divides, formed by locally derived alluvium, are identified by white bars perpendicular to former flow directions.

9 and ca. 5 Ma. Riquelme reported no buried soils, while Nalpas et al. (2008) reported zones of rubification and salt accumulation within the sedimentary accumulation. We observed a well-developed buried soil in a mining excavation of a Miocene gravel deposit (Naranjo and Puig, 1984), and recent work has examined several paleosols in Miocene deposits much further to the north (Rech et al., 2006). Whether these represent local hiatuses in deposition of this regional unit, or simply the ongoing lateral migration of streams, is not known. However the degree of soil development in some paleosols is suggestive of depositional hiatuses of 10^5 to 10^6 yr.

The termination of deposition is bracketed by interbedded ignimbrites near the surface and cosmogenic exposure ages of surficial cobbles. Along the Rio Salado (26°21′S, 69°53′W) Clark et al. (1967) found that the K-Ar age of a near-surface ignimbrite was 12.6 Ma, and that a nearby capping ignimbrite was 11.5 Ma.

TABLE 2. COSMOGENIC RADIONUCLIDE EXPOSURE AGES (THIS PAPER) AND PUBLISHED K/Ar OR Ar/Ar AGES OF ASH IN THE QUEBRADA LA NEGRA WATERSHED

Name	Latitude (°S)	Longitude (°W)	Altitude (masl)	^{10}Be concentration (atom g^{-1})	± (atom g^{-1})	^{26}Al concentration (atom g^{-1})	± (atom g^{-1})	^{26}Al/^{10}Be	±	^{10}Be minimum exposure age* (ka)	± (ka)	^{26}Al minimum exposure age* (ka)	± (ka)	Adopted minimum exposure age* (ka)	± (ka)	Maximum erosion rate (m m.y.$^{-1}$)
Cosmogenic radionuclide exposure ages of boulders and gravels on the surface of fluvial and alluvial landforms (this study)																
A-03-1	25.76	70.20	995	1.56E+07	1.9E+05	5.31E+07	1.6E+06	3.41	0.11	6290	580	2960	600	6290	580	0.01
A-03-2	25.76	70.20	999	1.55E+07	2.6E+05	4.60E+07	1.4E+06	2.97	0.11	6030	710	1730	140	6030	710	0.02
A-03-3	25.76	70.20	1005	1.62E+07	2.9E+05	3.67E+07	9.2E+05	2.27	0.07	Saturated	–	1060	50	>5170	–	0.00
ALT-04-1	25.76	70.20	1011	1.30E+07	2.0E+05	5.61E+07	1.9E+06	4.31	0.16	3100	120	>3120	–	>3120	–	0.01
ALT-04-2	25.76	70.20	1011	7.74E+06	3.2E+05	3.82E+07	1.4E+06	4.94	0.27	1250	70	1140	80	1190	80	0.32
ALT-04-7	25.76	70.21	995	5.91E+06	1.5E+05	2.79E+07	1.2E+06	4.72	0.23	890	29	699	43	790	130	0.58
ALT-2	25.76	70.19	1006	6.68E+06	1.9E+05	1.93E+07	6.1E+05	2.88	0.12	1030	40	423	17	727	430	0.81
AT-05-1	23.76	70.34	398	3.24E+06	1.3E+05	n.d.	–	–	–	776	37	n.d.	–	776	37	0.64
CAM-05-1	24.23	70.11	1259	1.25E+07	2.5E+05	5.29E+07	2.4E+06	4.25	0.21	2090	80	1650	190	1870	310	0.16
CG-04-1	24.68	69.88	2133	3.20E+07	9.8E+05	1.16E+08	2.9E+06	3.64	0.14	4770	650	3260	680	4770	650	0.03
CG-05-1	24.85	69.88	2139	3.58E+07	1.4E+06	1.20E+08	3.9E+06	3.34	0.17	Saturated	–	Saturated	–	Saturated	–	0.00
CHM-05-1	24.03	69.77	1010	1.47E+07	3.4E+05	4.35E+07	2.1E+06	2.96	0.16	5220	620	1610	190	5220	620	0.02
CHM-05-2	24.05	69.81	960	1.32E+07	2.5E+05	4.84E+07	2.0E+06	3.68	0.17	3930	240	2550	520	3930	240	0.05
CLS-06-2	23.76	70.44	90	1.50E+05	1.6E+04	8.91E+05	3.9E+05	5.92	2.66	38	4	34	15	38	4	16.0
CRC-06-1	23.62	70.31	583	1.92E+06	6.5E+04	1.03E+07	8.0E+06	5.38	4.15	363	14	309	286	336	38	1.61
CRC-06-2	23.62	70.31	583	1.48E+06	4.6E+04	9.46E+06	5.6E+05	6.39	0.43	274	9	280	19	275	8	1.99
MLG-04-1	25.77	70.03	1272	1.75E+07	4.6E+05	7.16E+07	2.7E+06	4.10	0.19	4160	390	Saturated	–	4160	390	0.00
Y-03-1	24.1	70.02	1024	1.13E+07	1.5E+05	4.59E+07	1.5E+06	4.05	0.15	2420	70	1790	170	2110	440	0.13
YNG-05-2	24.1	70.02	1014	1.02E+07	2.2E+05	3.90E+07	1.7E+06	3.83	0.19	2010	80	1260	110	1640	540	0.21
YNG-05-4	24.1	70.02	1014	6.27E+06	1.2E+05	3.10E+07	1.6E+06	4.95	0.27	988	25	846	67	917	100	0.48
YNG-3	24.1	70.02	1014	9.08E+06	1.3E+05	3.42E+07	1.0E+06	3.77	0.12	1670	40	992	50	1330	480	0.30

K/Ar and Ar/Ar ages of ashes found in Pliocene fluvial sediments (published)

Latitude (°S)	Longitude (°W)	Method	Age (Ma)	± (Ma)	Reference
23 22.157	69 33.581	K/Ar biotite in ash	0.6	0.4	Basso (2004
23 22.722	69 24.732	K/Ar biotite in ash	0.7	0.3	Marinovic and García (1999)
24 6.859	69 21.661	K/Ar biotite in ash	1.5	0.3	Marinovic et al. (1992)
24 13.549	70 6.578	Ar/Ar sanidine in ash	2.1	0.1	Ewing et al. (2006)
24 2.655	70 15.929	K/Ar biotite in ash	2.4	0.3	Marinovic et al. (1992)
23 31.075	70 15.080	K/Ar biotite in ash	3	0.2	González and Niemeyer (2005)
24 30.088	69 39.104	K/Ar biotite in ash	3.4	0.9	Marinovic et al. (1992)
23 37.365	69 56.477	K/Ar biotite in ash	4.4	0.5	Cortés (2000)
24 8.541	70 0.260	K/Ar biotite in ash	4.6	0.6	González and Niemeyer (2005)
23 44.246	70 18.870	K/Ar biotite in ash	5.2	0.5	González and Niemeyer (2005)
24 38.946	69 6.904	K/Ar biotite in ash	5.4	1.6	Marinovic et al. (1992)
23 26.366	69 12.202	K/Ar biotite in ash	11.8	0.6	Marinovic and García (1999)
23 24.315	69 44.727	K/Ar biotite in ash	20.1	1.1	Basso (2004)

*Calculated using a mean attenuation length of cosmic-ray interaction of 165 g cm^{-2}, a sample density of 2.70 g cm^{-3}, a ^{10}Be production rate of 5.10 atoms g-quartz^{-1}, a ^{26}Al production rate of 34.07 atoms g-quartz^{-1}, and assuming muon contribution of 1.50% at sea level.

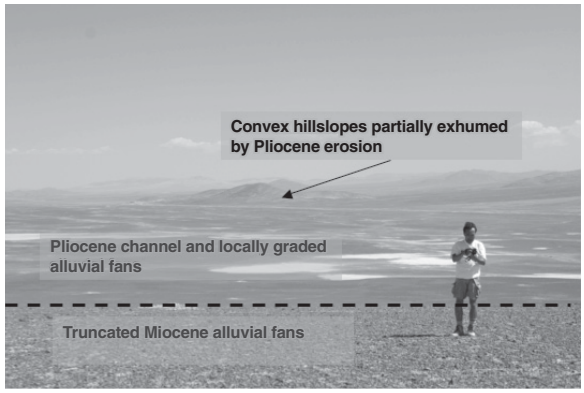

Figure 7. Photograph, facing the SW from Miocene terraces near Aguas Blancas. The photo shows the well-preserved Miocene surfaces, the deeply incised Pliocene channels, and fans graded to those channels. The light-toned features on the Pliocene surface are Quaternary aqueous deposits and channels.

To the south, near Copiapo, these authors found that tuffs under the geomorphic surfaces were in the range of 9–9.5 Ma, suggesting what must be expected to be regional variability in the deposition of the surficial-most layers. Near El Salvador, a few kilometers NW from the Rio Salado, Nishiizumi et al. (2005) found surface exposure ages of cobbles on alluvial deposits to range from ca. 4 to 9 Ma. In this study, we sampled cobbles from many terraces and alluvial deposits for exposure age dating. A cobble from a prominent ancient alluvial surface within the Pampa Grande (sample CG-05–1; Table 2) was saturated with respect to ^{10}Be and ^{26}Al, indicating exposure times exceeding ~7.1 m.y. Further to the north, a high-standing unit mapped as Tpm (Oligocene–Miocene Formacion Pampa de Mulas) gave a ^{10}Be exposure age of 5.2 Ma (sample CHM-05–1; Table 2). While more mapping and dating are required to fully understand the Miocene units, it is likely that they represent multiple stages of infilling, concluding between ca. 11 and 5 Ma.

Figure 9A shows the reconstructed Miocene basin fills of a major portion of the watershed (geologic map quadrants Aguas Blancas, Palestina, and Baquedano). Given that Miocene geomorphic surfaces rise above incised Pliocene landforms by tens to hundreds of meters in certain locations, the basin reconstruction results in a substantial burial of parts of the basin, including small hills and ridges in the present landscape (compare Figs. 9A and 9C). These hills, which today are well rounded and convex, may be partially (or wholly) relict landscape features formed prior to Miocene burial, possibly in the Oligocene. This seems also true for the landscape in Figure 8. The absence of significant Miocene erosional features suggests that the Miocene phase primarily consisted of basin infilling, while the post-Miocene periods have largely involved excavating this accumulated sediment and exposing a largely pre-Miocene topography. For example, we found the elevational differences between the straths (Miocene) and the valley floor (latest Pliocene) shown in Figure 8 to be 94 m and 46 m for the upslope and downslope strath terraces, respectively. These local incision amounts (which should be equal to the depth of excavated sediment) are within the ranges reported in Figure 9B. While it may be argued that some hillslope erosion and subsequent morphological evolution may be due to post-Miocene incision and re-exposure, the exceedingly low bedrock erosion rates (~<1 m m.y.$^{-1}$; Owen et al., 2010) argue against much post-Miocene landform modification.

The reconstructed Miocene landscape indicates a regional slope of geomorphic surfaces that directed drainage through prominent canyons toward La Negra, or around the mountainous ridge to the NE, and then again toward La Negra. Given the regional compressional tectonic regime caused by plate convergence and subduction, topographic changes since Miocene times seem likely. Lamb and Hoke (1997) proposed a general westward tilting (3°) of the forearc near Iquique, north of our study area. To the south, at the Rio Salado (27°S), Riquelme et al. (2007) estimated a maximum post-Miocene westward tilting of the landscape of 1.3°. Recently, Jordan et al. (2010) examined the deformation history of the Calama Basin, to the north of our study area, concluding that there has been 1.3° of western tilting of the basin since the Miocene. This tilting has certainly caused stream incision, and Riquelme et al. (2007) suggested this as the cause for the deep canyon of the Rio Salado. However, as we will discuss later herein, while there is deep incision of Miocene sediments in our field area, there is a profound cessation of incision in the late Pliocene that appears so regionally pervasive that it would seem to be unrelated to tilting or faulting history.

Pliocene fluvial deposition and erosion. Miocene deposits are significantly incised or buried by younger deposits mapped as mainly Pliocene in age (units Tas or MPla; Marinovic et al., 1992; Cortés, 2000; González and Niemeyer, 2005). These deposits also record river flow paths similar to channels that deposited the older Tertiary gravels, and through canyons now blocked by alluvial fan–derived drainage divides.

In Figure 9C, the Pliocene landscape is reconstructed, illustrating the incision that occurred between the Miocene and late Pliocene.

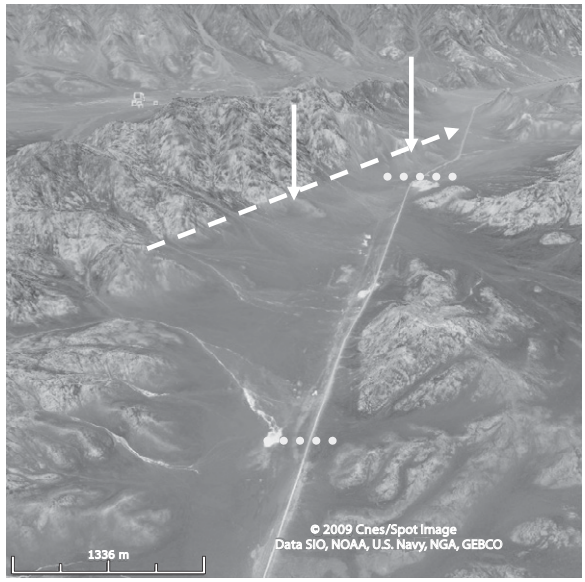

Figure 8. An oblique (facing west) Google Earth view (vertical exaggeration of 3×) of a Pliocene canyon (left portion of upper dashed line in Fig. 3A) showing two identified plausible Miocene strath terrace remnants. White solid arrows show approximate straths, and dashed white arrow shows the slope and trajectory of the presumed channel. A Mesozoic continental sandstone clast fragment (exotic to the area) was found on the terrace closest to forefront. Note the dark, roughly subparallel bands on upland hillslopes ("zebra stripes) composed of sorted silicic fragments. Light-toned areas between stripes are largely surface exposures of underlying gypsum/anhydrite-rich soils. The alluvium-derived drainage divides, shown in Fig. 6, are illustrated here (based on topographic maps) as dotted lines.

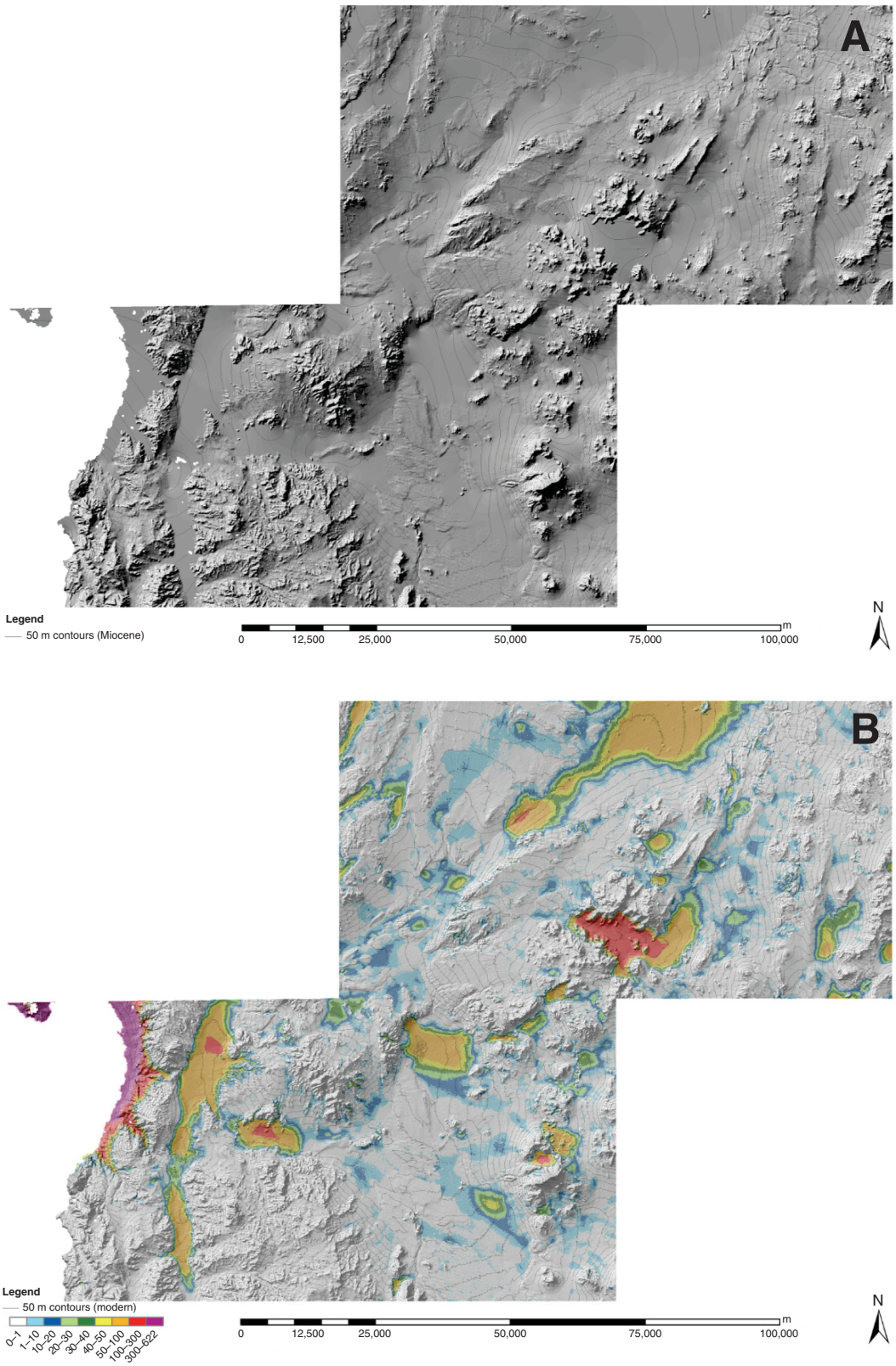

Figure 9 (*on this and following page*). (A) Topographic reconstruction of the Miocene landscape for the drainage of the Quebrada La Negra, (B) the amount of incision between the Miocene and Pliocene.

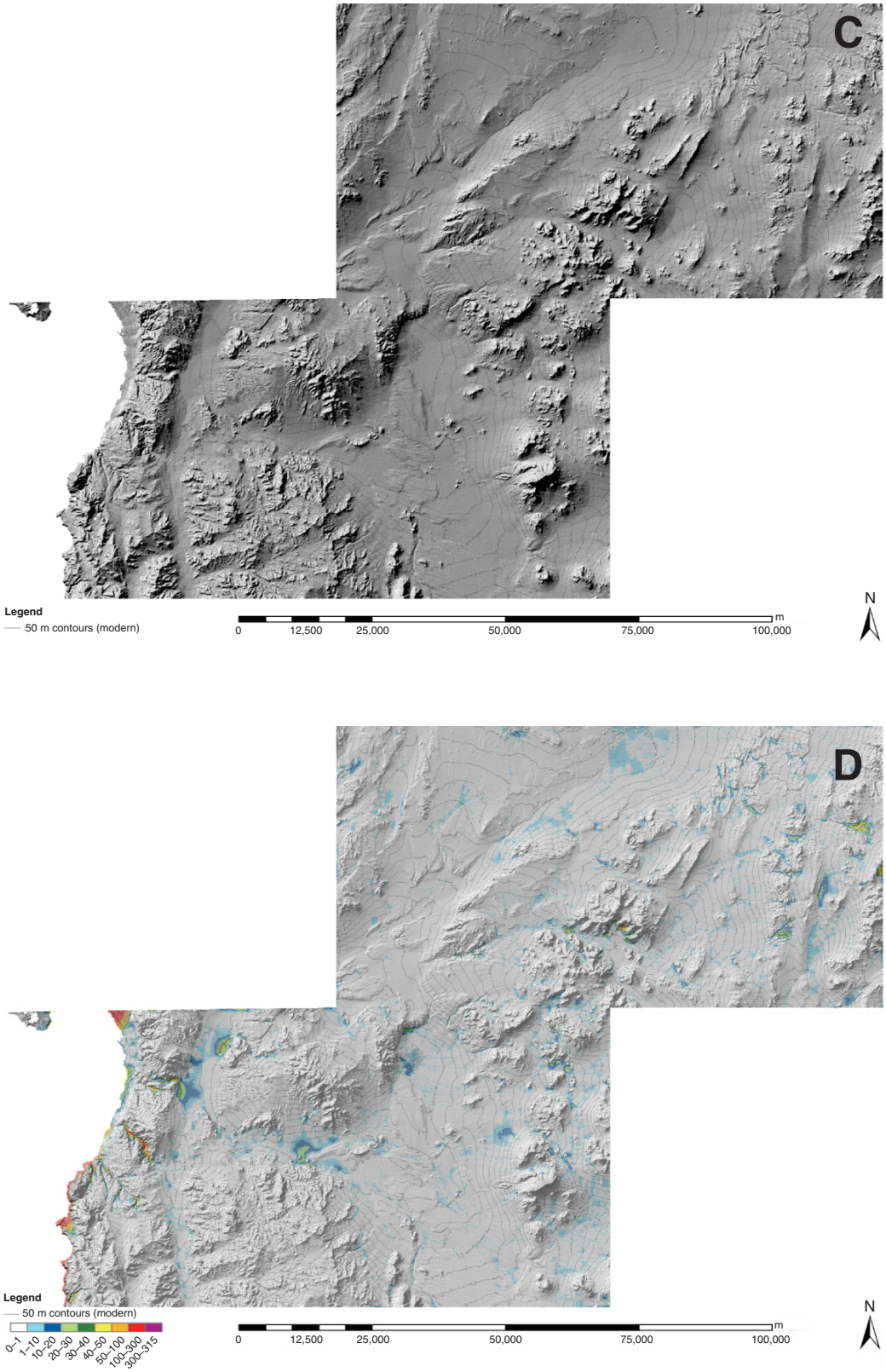

Figure 9 (*continued*). (C) the Pliocene topography of the area, and (D) the amount of incision between Pliocene and today

This difference map (Fig. 9B) shows that incision increases with distance upslope, as noted by others (Riquelme et al., 2007). For the survey area, the total average Miocene to Pliocene incision is 13 m, with a range of 0–620 m.

The beginning of this post-Miocene incision is unknown. It must postdate some of the youngest exposure ages of ca. 5–6 Ma. Additionally, the erosion must have terminated by ca. 2.1–2.4 Ma based on ages of near-surface ash beds and cosmogenic exposure ages of surface boulders and quartz (Table 2). The large volume of sediment eroded from the preexisting Tertiary gravels also suggests a multi-million-year episode of erosion/deposition. For the field area we have reconstructed, the volume of post-Miocene incision averages 12.5×10^{-3} km^3 km^{-2} over the area studied (Table 3).

Mortimer (1980) and Riquelme et al. (2007) proposed that incision into the Atacama gravels (and related Miocene deposits) was caused by either tectonic uplift or by climate change. Mortimer discounted tectonic mechanisms, noting that uplift and warping of stream channels occurred throughout the Tertiary interval of gravel deposition, and that streams generally planed off these offsets and maintained their gradient. There are numerous fault offsets in Miocene sediments throughout our field area, with a particularly large (~100 m) relative downdropping on the western side of the Falla Boquete, upstream of the Salar Navidad (which now captures all drainage from the Aguas Blancas quadrangle). While this downdropping certainly

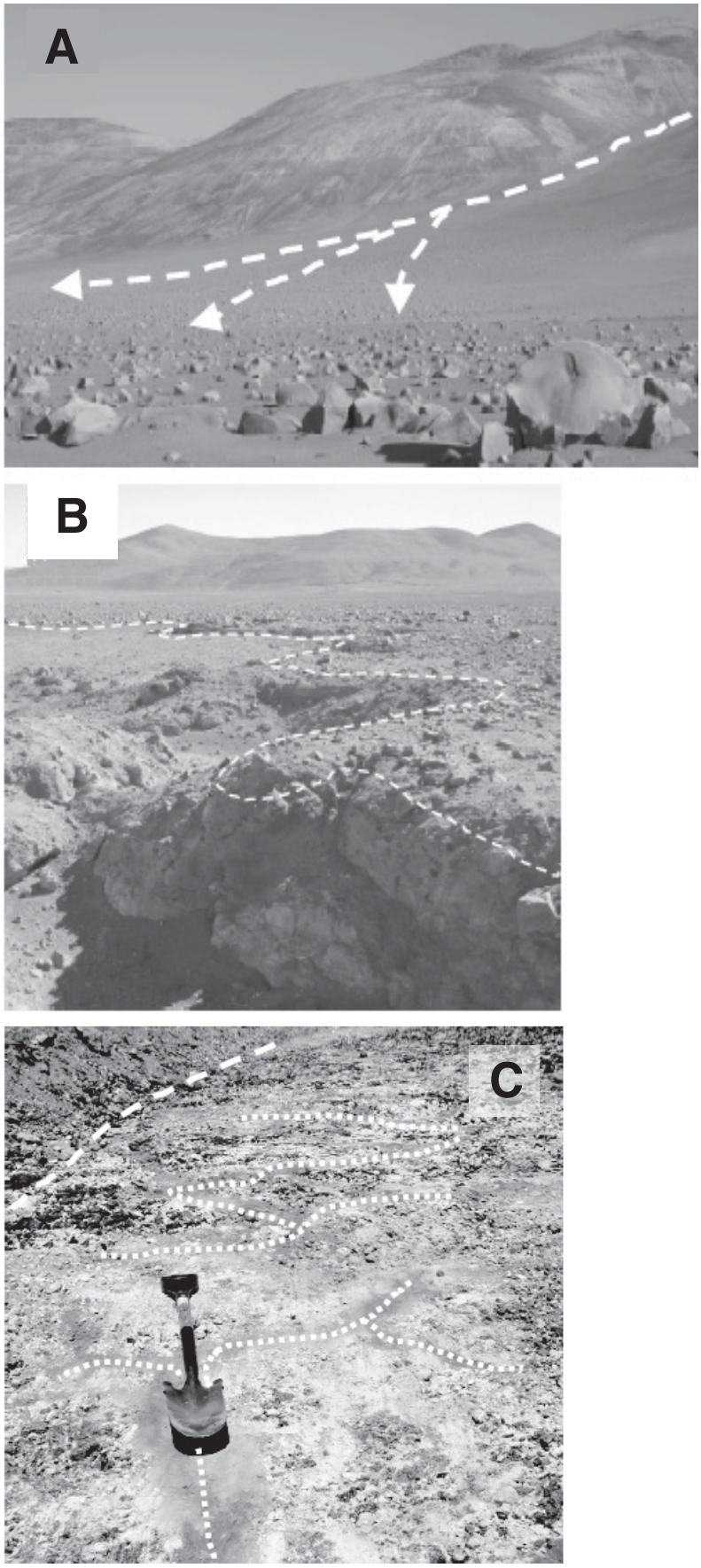

Figure 10. (A) Photograph of canyon in upper left portion of Figure 6A and rear of Figure 8, showing late Pliocene–aged local alluvial fans, local ventificated debris flows, and inactive and salt/dust-infilled source channels. White dashed line shows salt/dust-infilled channel that supplied the debris flow. The boulders float on soil impregnated with dust and salt and shown as in (B), a photograph taken in an exposure ~30 km west of A. Dotted line in B denotes area where construction has removed the surficial "boulder field," revealing a largely gravel-free, salt-rich soil below. (C) Photograph of steep convex hillslope (upslope is in background) where soil layer has been removed by bulldozer (berm line illustrated by white dashed line). Polygonal cracks (identified by dark soil tones and white dotted lines) have extended from the overlying soil into the underlying fractured (but saprolite-free) bedrock. Both the large boulder in A and the exposure in B are about 1 m.

TABLE 3. CALCULATED POST-MIOCENE WATERSHED CHANGES

Time interval	Drainage area (km^2)	Time (m.y.)	Min/max incision (m)	Average incision (m)	Maximum relief (km)	Total erosion (km^3)	Erosion ($km^{-3}\,km^{-2}$)	Erosion rate ($km^3\,m.y.^{-1}$)	Discharge ($km^{-3}\,yr^{-1}$)
Miocene–Pliocene	11,160	3.9	0/622	12.6	4	140	1.25×10^{-2}	35.9	182.0
Pliocene–Modern	11,160	2.1	0/315	1.1	4	13	1.16×10^{-3}	6.2	0.6*

Note: Incision rates and volume were calculated by digital elevation analyses described in text. Changes in discharge use locally adjusted relationship of Syvitski and Milliman (2007).
*Assigned value.

altered the stream gradients, it did not reverse flow and did not cause the present internal drainages that characterize much of the watershed. Mortimer (1980) hypothesized that a post-Miocene aridification (ceasing gravel deposition) was punctuated by an increase in precipitation that initiated downcutting—a trend that has continued, in his view, despite subsequent climate changes. Mortimer (1973) termed this post-Miocene landform development as his stage 4 (and final) set of landscape erosional processes. Near Aguas Blancas (Fig. 3A), the channels that were active in the early Pliocene and were effective pathways for sediment transport toward present-day Antofagasta are now all veneered with late Pliocene (and some younger) sediments from local drainages. These local fans create drainage divides (Fig. 6A), and some local fans drain in directions *opposite* to the earlier Pliocene channel paths. Despite an abundance of evidence for faulting throughout the region, we see no fault scarps of sufficient magnitude or linear patterns in these drainages to suggest that tectonics caused this drainage change. Another regional geomorphological feature is stream capture. We note that the present channel from Aguas Blancas is a very narrow, deeply incised channel that apparently represents the upslope propagation of a late Pliocene or younger stream capture by the drainage system that lies to the north (Fig. 6C). However, stream capture is insufficient to explain the profound fluvial and geomorphic changes that appear to have ensued roughly at the end of the Pliocene. In addition, this channel itself now terminates downstream in the Salar de Navidad. Later herein, we present observations suggestive of a fundamental change in climate, one that changed geomorphic processes at all scales across the landscape from pre–late Pliocene conditions.

Post-Pliocene stream activity. Figure 9D shows the calculated stream incision from the end of the Pliocene to the present. The striking feature of this reconstruction is the exceedingly modest erosion during the Quaternary compared to that which occurred earlier. The total average Quaternary incision is ~1.1 m (range of 0–315 m), and the total volume of sediment removed is 1.2×10^{-3} km^3 km^{-2} (Table 3).

As discussed earlier, the stream trajectories of the Quaternary drainages differ greatly from that in the Miocene and early Pliocene. Blocked drainages, channel abandonment/inactivity, stream capture, and development of internal drainage are all characteristics of the post-Pliocene landscape.

Interpretations of Late Pliocene to Quaternary Landscape Features

Evidence for climate change from inferred changes in stream discharge and sediment mobilization. Stream capture may have changed the hydrological flow through one or more canyons, and therefore assisted in the accumulation of localized sources of sediment from nearby mountains. This mechanism does not explain why the diverted streams did not maintain a prediversion flow and erosional capacity, and why throughout the entire watershed (except to the east, where remnants of Tertiary fans remain above the Pliocene fill) all mountain ranges are flanked almost exclusively by late Pliocene or early Pleistocene fans that grade onto largely hydrologically inactive early Pliocene channels or deposits (Fig. 6). We hypothesize that sometime earlier in the Pliocene or late Miocene, an increase in regional precipitation and/or regional tilting led to the onset of incision into the landscapes dominated by Miocene gravels. This incision led to the erosion and redistribution of large quantities of sediment. The depth and width of incision in the entire watershed are suggestive of effective water flow and sediment transport to the sea. The total volume of Miocene sediment removed totals ~140 km^3 (Table 3).

The geomorphic features indicate that near the end of the Pliocene, a climatically induced decline in water flow led to channels that became ineffective in removing locally derived alluvium. Throughout the region, local alluvial fans aggraded and overtopped adjacent Pliocene stream channels. The deposition of this local material ceased ~2.1 m.y. ago (in the early Pleistocene), based on near-surface ash deposits throughout the region and from cosmogenic exposure ages (Table 2). The total quantity of sediment removed since the Pliocene (in our study area) is 13 km^3.

If this large change in landscape incision and hydrology is due to climate, as we propose, how can the landscape reconstructions be used to estimate quantitative changes in precipitation? Syvitski and Milliman (2007) presented an analysis of a large number of drainages from around the world, and they developed an empirically based relationship between a number of watershed features (included discharge) and the average erosion rate:

$$Y_s = \omega B Q^{0.31} A^{-0.5} R T \,, \qquad (4)$$

where Y = average erosion in watershed (MT km^{-2} yr^{-1}), Q = water discharge (km^3 yr^{-1}), A = drainage area (km^{-2}), R = maximum relief (km), T = mean average temperature (°C), and ω (~0.0006) and B (~1) are parameters for geology, human impacts, etc. From the end of the Pliocene to the present time in our watershed, we have measured all parameters except discharge. Houston (2006) reported discharge rates of 1–12 $m^3\,s^{-1}$ for streams in northern Chile reaching the ocean. Acknowledging human uses of water resources, we used a somewhat arbitrary baseline of 20 $m^3\,s^{-1}$ in these calculations. These approximate discharge rates, with the watershed size of our study, fall well below the regressions between drainage area (x axis) and discharge (y axis) in Syvitski and Milliman's (2007) derivation of the empirical relation above. For comparative purposes, we simplified Equation 4 by combining all constants into a single term (K): $Y = KQ^{0.31}$.

Using the apparent Pliocene to modern sediment removal, and the approximate discharge of current Atacama Desert streams, we estimated the K value. This K value, along with apparent Miocene to Pliocene sediment removal, was used to estimate the Miocene to Pliocene discharge rate. There are several assumptions implicit in this calculation: (1) the extrapolation of Syvitski and Milliman's (2007) empirical relationship to much drier conditions is still valid; (2) the bulk of sediment removal from a watershed for a given period is largely from basin fills rather than hillslopes; and (3) changes in sediment availability are not the cause of the reduction in sediment removal with time. As for item 3, while much Miocene sediment was removed between the end of the Miocene deposition and the end of the Pliocene, large tracts of Miocene sediment still remain, and additionally, Pliocene alluvial fans are deposited along mountain fronts. Thus, there seems

ample sediment (of both Miocene and Pliocene age) available for removal if climatic conditions are suitable. With respect to item 2, it is likely that during all periods of basin excavation, sediment derived from hillslopes contributed to the total mass loss in the drainage basin. By focusing only on the removal of alluvial sediments (it is impossible to reconstruct or estimate sediment loss from hillslopes between different time intervals), we are systematically underestimating basin sediment loss. It is arguable that the underestimation is proportional for both the Miocene–Pliocene and Pliocene–present time intervals, and focusing only on basin sediment removal provides a valid comparison. Finally, it is certainly debatable whether it is correct to extrapolate the global discharge versus erosion model to such dry conditions. However, since all parameters in the model remain constant over the entire period of consideration, the only variable capable of the large differences in sediment loss is thus discharge. However, the numerical differences between time intervals may be best viewed as semiquantitative given the climatic uniqueness of this drainage basin. In that vein, the measured changes in erosion can be viewed more qualitatively as a measure of changes in the "erosion intensity", I_e, (Montgomery et al., 2001):

$$I_e \sim QS,$$

where Q = discharge (area × precipitation) and S = slope. The apparent difference in erosion intensity from Miocene to modern times, which is also linked with discharge, is also suggestive of significant decline in precipitation.

The results suggest that the present discharge is ~280× smaller than the Miocene-to earliest Pleistocene (6–2.1 Ma) discharge (Table 3). Alternatively, if the erosion occurred over a period from 9 to 2.1 Ma, the apparent decline would be ~50×. This is a surprisingly large apparent change in precipitation, but we will show other geomorphic features that also reveal significant declines in available water.

Local Pliocene Debris Flows on a Currently "Frozen" Landscape

The late Pliocene alluvium that interfingers with and overlaps the channel deposits possesses characteristics fundamentally different from deposits formed by post-Pliocene fluvial processes. Pliocene fan sediments commonly contain streams or fields of cobbly to bouldery material having particle sizes that can only be attributable to debris flows (Fig. 10A). We found no such deposits on post-Pliocene surfaces. In addition we found that: (1) the boulders are heavily varnished or, in areas of high wind trajectories, heavily ventificated (Fig. 10A); (2) the boulders lie on salt-rich, nearly gravel-free, soil horizons and thus "float" on the land surface in a manner completely analogous to desert pavements in the Mojave Desert (McFadden et al., 1988) (Fig. 10B); and (3) the source areas for the sediment (hillslopes) are now entirely mantled with salt-rich soils (anhydrite, gypsum, halite, natratites, etc.) that show no evidence of debris activity (Fig. 10A). Modern hillslope channels do not exhibit any evidence of recent boulder transport, and many are ineffective at the removal of eolian salt and dust.

These field relationships occur discontinuously (depending on the size, mean slope, and lithology of the watershed) from Antofagasta (~23.5°S) to the vicinity of Taltal (Fig. 1) (~25.5°S). At the latitude of present-day Chanaral (~26.5°S), hillslopes are largely denuded of salts and dust. This suggests that a rainfall threshold has been exceeded, which in turn facilitates fluvial processes capable of removing fine materials from slope surfaces. This observation is supported by erosion rates based on cosmogenic nuclide measurements. Rates of soil production (bedrock conversion to a mobile soil mantle) are about ≤1 m m.y.$^{-1}$ near Antofagasta, increase to 2–3 m m.y.$^{-1}$ at Chanaral, and are up to >20 m m.y.$^{-1}$ at La Serena (120 mm MAP; Table 1). Present rates of bedrock conversion to soil are strongly linked to rainfall, and the rates in the Aguas Blancas region are among the lowest rates yet reported on Earth. Erosion rates this slow produce only bouldery debris. In the salt-rich landscapes such as these, the boulders may be shattered by salt weathering during the denudation process. Debris flows also require sufficient water to mobilize granular mass and cause it to travel hundreds of meters onto fan surfaces. The lack of post-Pliocene debris-fan deposits also points to significant drying and arrival of salt-rich soils.

Rehak et al. (2010) examined the variation of a number of features of the Andean drainages in northern Chile. They observed a dramatic decline in stream and drainage density north of ~27°S. These authors attributed this boundary to the northward-most migration of Pacific westerlies in Pleistocene pluvial periods, and to the related boundary in alpine glaciation. It is interesting to note that the lower-elevation landscapes we examined, unaffected by glaciation, show striking changes in soil and geochemistry. We recognize the potential impact of past climatic oscillations on the landscape, but we also later suggest that these oscillations may be experienced at all latitudes, and thus are part of a long-term and pervasive climate signal on numerous landscape features that is reflected in each latitudinal belt.

Development of Hillslope Soils Under Decreasing Precipitation

Our research on hillslope soils in and around the Aguas Blancas region reveals processes that fundamentally differ in character from other terrestrial settings. Briefly, soils on convex portions of hillslopes in semiarid to more humid regions reflect ongoing balance of slope-dependent erosion (driven largely by biotic agents such as burrowing animals, ants, tree-throw, etc.) and conversion of underlying rock to soil (e.g., soil production; Dietrich et al., 1995; Heimsath et al., 1999). The result of these processes, at steady state, is that soil thickness decreases with increasing slope curvature, and soil production (from underlying rock) increases with curvature. In the present hyperarid Atacama Desert, in contrast, processes not observed in more humid regions magnify themselves and result in unique patterns indicative of extreme, and lengthy, hyperaridity.

Near Aguas Blancas, we have found that a significant amount of soil mass on hillslopes is composed of sulfates and other salts and dust that must be (~50% or more of volume) derived from atmospheric deposition. On nearly level fans that adjoin these hillslopes, these salts and the dust are vertically reorganized by small stochastic rainfall events, with more soluble components leaching downward (Ewing et al., 2006, 2008b). The resulting soil profiles, which vary from a few centimeters to more than 150 cm in thickness, contain sulfate polygons and seams that can permeate into the underlying sediment or bedrock. Field observations suggest that over long time periods, the physical movement and turbation of these salts (which produce and move the prisms) succeed in slowly fracturing the rock and moving it into the soil profile (Fig. 10C). The means of soil production is both abiotic and physical, the latter being by salt weathering and heaving. Downslope soil transport occurs slowly and is facilitated by salt dilation and creep. There are rare surface runoff events that generate sheetwash and rills. In this area, our observations evince two dramatically different landscapes, but they are both still present. The previously active bedrock source areas for Pliocene alluvial fans and debris flows are now essentially "frozen" in Quaternary salt.

Between the present villages of Taltal and Chanaral, the character of hillslope soils, as well as soils on nonsloping land surfaces, undergoes a fundamental change compared to landscapes to the north. Sulfate in soils of all slope positions declines greatly due to increased rainfall, and carbonates become the dominant secondary mineral (Quade et al., 2007) in soils as plant density (and resulting soil CO_2 concentrations) increases. Despite the increase in moisture and

its ability to leach salts, rainfall is generally insufficient to support vascular plants, which are critical to maintaining a soil cover of silicate material derived from underlying rock. As a result, hillslopes become nearly soil free, e.g., erosion rates are greater than the soil production rates. This pattern occurs discontinuously from slightly north of modern Chanaral (~26°S) to the region between present-day Copiapo (~27.4°S) and Vallenar (~28.6°S) in the coastal range and nearby Central Depression. The west-to-east extent of this belt is unknown. At those more southerly latitudes, continually increasing rainfall facilitates a greater plant density, and there is correspondingly greater soil production. We propose that the modern "soil-free" latitudinal zone, which corresponds with the observations of active (but slow) bedrock erosion and sediment transport, likely represents an approximate analog for climatic and geomorphic conditions that existed nearly 400 km to the north in the latest Pliocene or early Pleistocene, when the hillslopes in the Aguas Blancas region were apparently stripped to saprolite-free bedrock, and the sediment that was removed filled and blocked local drainages (Owen, 2009).

While the present region 400 km to the south of Aguas Blancas may represent the final stages of fluvial processes that occurred in the Pliocene, we hypothesize that this soil removal process began with hillslopes mantled by silicate soil. This implies a climate condition more humid than present-day Chanaral and possibly close to that of La Serena, i.e., one that could support enough soil production and vegetation to maintain a soil cover. The Pliocene fluvial channels around Aguas Blancas (Fig. 6A) would certainly have required considerable moisture in order to develop their morphology. Presently, from Vallenar to La Serena (28.5°S to 30°S), hillslopes are mantled with silicate rock–derived soil, and the soil-bedrock interface is commonly characterized by saprolite rather than fresh bedrock (Fig. 5B).

We hypothesize that hillslopes in the Aguas Blancas region were mantled with rock-derived soils sometime from the late Miocene to early Pliocene. These soils would have also supported at least a partial vegetative cover. We do not have any further chronological constraints on this time period. It is consistent, however, with work by Hartley and Chong (2002), who suggested that semiarid climates existed in the region between ca. 6 and 3 Ma. A general climatic degradation then resulted in the loss of plant cover and increased erosion rates from rock, rates that greatly exceeded soil production rates. These stripped soils and rocks were deposited as coalescing alluvial fans that now apron the mountain ranges and cover, or partially cover, formerly active stream channels. The final phase of this aridification, which was manifested after the hillslopes were denuded and nearly made soil free, was the slow accretion and partial redistribution of atmospheric salts with the accompanying salt weathering. These salty soils now blanket all landscape positions. The chemically unaltered soil-bedrock interfaces in these salt-mantled hillslopes support this interpretation. There is a factor of 35 difference in MAP between present-day Antofagasta (3.5 mm yr^{-1}) and La Serena (119 mm yr^{-1}), consistent with the relative changes in discharge implied by erosion rate changes in the Quebrada La Negra watershed.

In summary, the sedimentological and hillslope soil evidence in the hyperarid region suggests a decline in rainfall of ~100 mm yr^{-1}, if we use the present landscape of Chile as an analog.

Post-Pliocene Fluvial Activity and Stream Profile Development

Post-Pliocene fluvial activity is minimal, except where tectonic uplift (relative to sea level) and periodic sea-level fall in the Pleistocene have led to local steepening of channels and incision (e.g., Mortimer, 1973, 1980). The stream channels that cross the Coastal Cordillera become increasingly convex upward with decreasing latitude and rainfall (Fig. 11A). This convexity suggests increasing channel disequilibrium with decreasing latitude and rainfall. As illustrated in Figure 2B, there is little evidence to suggest that significant differences in present uplift are the cause (though the rates may have changed over time). We accordingly focus on the question of whether the profiles reflect the effects of post-Miocene aridification.

As discussed in the Methods section, we examined three scenarios for the channel long profile shape (Fig. 11B). First we assumed that the channel was once at equilibrium. Second, if climate change was responsible, the change from a previous steady state to the present shape must have occurred in roughly <10 m.y. (e.g., post–Atacama Gravel deposition). The three experiments are listed next and are discussed in order.

Experiment 1. Channels due to decreased K only: We progressively decreased K to obtain the coast range convex shape, while keeping U constant. This required a reduction of K by a factor of 50 over 50 m.y. Thus, while the relative decline in the value of K (50×) is roughly consistent other climatic indicators discussed in this paper, the time required is too long to be reasonable.

Experiment 2. U was progressively increased to match the profile shape, while keeping K constant: This experiment required an increase of U on the coast side by a factor of 18 over 20 m.y., while in the middle and eastern sections, factors of 1.1 and 2.75 were sufficient. The time frame for this is likely too long, and we have no information to suggest that the uplift rates have increased by such large factors over time.

Experiment 3. Progressively decreased K while increasing U: This experiment resulted in the best reconstruction of the profile. We reduced K by a factor of 10 and increased U by factors of 3.5, 1, and 2.25 (from west to east) over 10 m.y. Both the reductions in K and increases in U are relatively modest and geologically feasible, as is the time frame required for the changes to occur.

While the numerical models are at best an approximation of the many processes that may contribute to the channel shape, they do show that broad aspects of river channels after a long change in erosivity, and modest increases in uplift rates can indeed result in convex-up profiles in a matter of a few million years. The way in which the reduction in the value of K translates into real climate and rainfall differences is not known, but it does reinforce our interpretation that northern Chile has been geomorphologically and geochemically adjusting or relaxing to large reductions in rainfall since at least the Pliocene.

Evidence for "Extreme" Post-Pliocene Precipitation Events (Punctuated Hyperaridity)

While we conclude hyperaridity has extended since the late Pliocene or early Pleistocene, there is ample pedological and geomorphic evidence for rainfall events, or cycles, that exceed the present day "norm." The pedologic evidence is the depth distribution of salts in the Pliocene soils: thick sulfate layers over nitrate/chloride-rich horizons to depths of 150 cm or more (Ewing et al., 2006). While this sequence is clearly reflective of extreme aridity (and inability to remove deposited salts), the depth of the accumulations cannot simply be explained by the "average" precipitation events, and must reflect relatively rare (but relatively large) rainfall events. We performed simple numerical models akin to those of Mayer et al. (1988) for soil carbonate (data not shown here), and they reveal that these salt profiles can form from centennial to millennial rainfalls of several centimeters or more, allowing the effective dissolution of near-surface halite and its transport to depths exceeding 1 m. However, while it seems the soil profiles must require these occasional rainfalls, they are infrequent enough to that they do not exceed a threshold that would ultimately remove this salt from the landscape.

The geomorphic evidence for brief and/or infrequent periods of relatively large precipitation

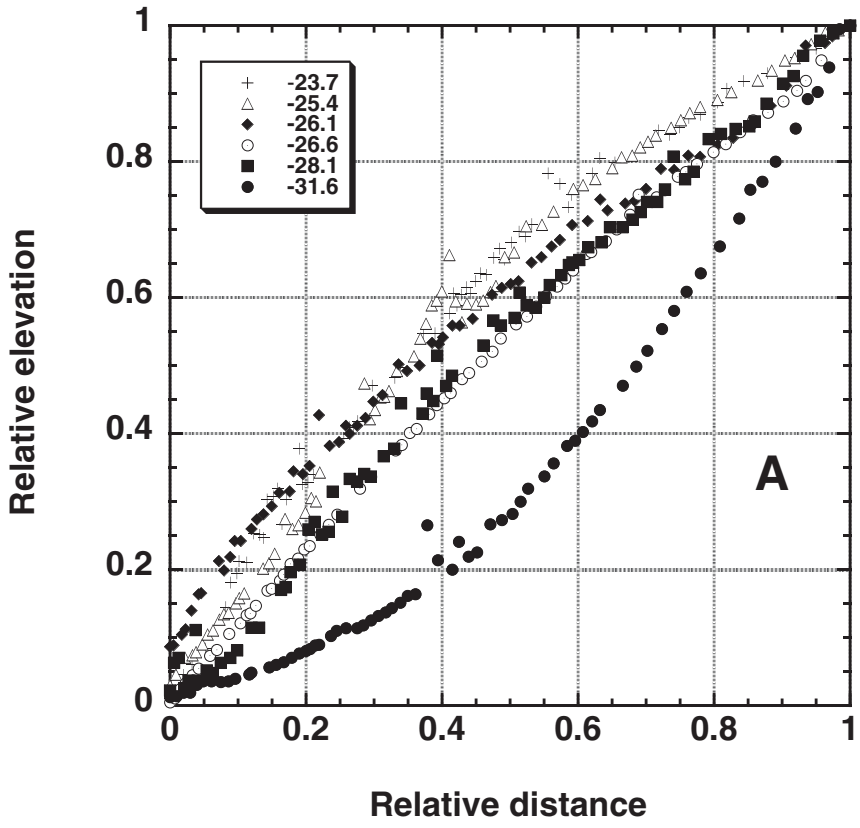

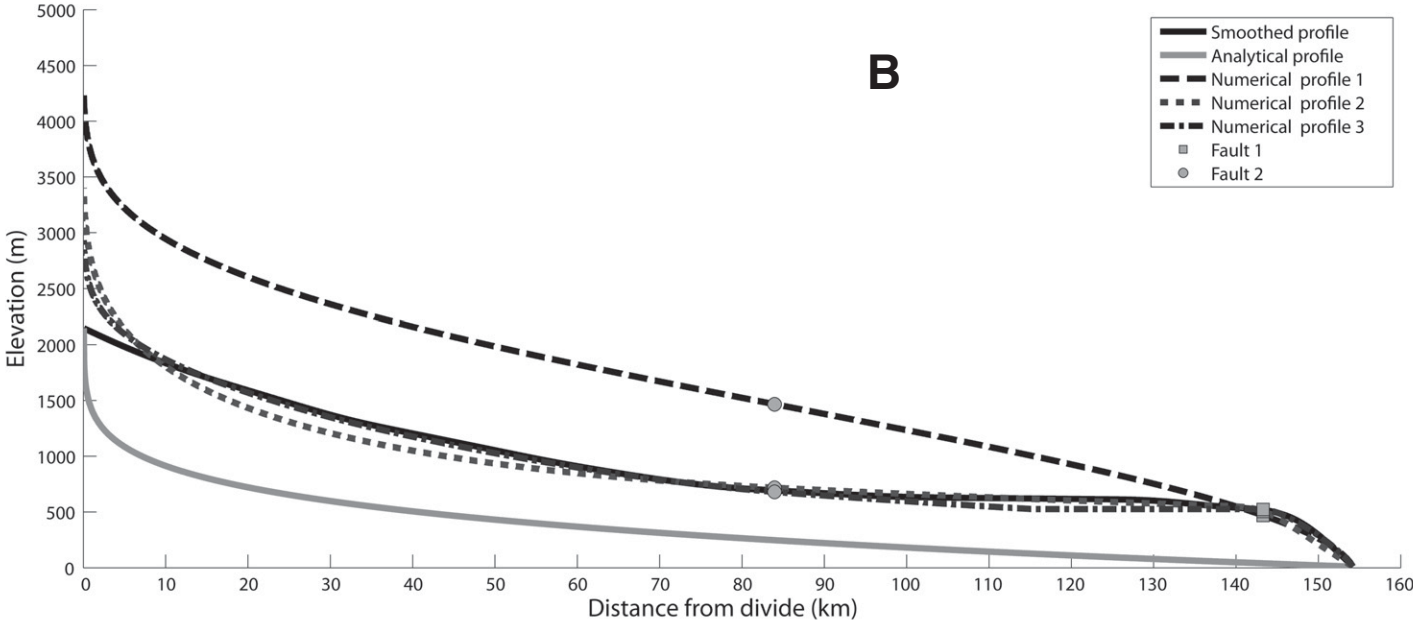

Figure 11. (A) Normalized stream profiles of channels, arranged by latitude, that traverse the Coastal Cordillera in northern Chile. (B) The measured long profile of the Quebrada la Negra and its potential steady-state profile, and results of numerical modeling experiments of differing combinations of increases in uplift and decreases in erosivity. The experiments are described in the text.

events is manifested in sediment reworking on both hillslopes and more gently sloping surfaces like alluvial fans. In the hyperarid zone, a nearly universal soil surface pattern on hillslopes consists of contour-oriented gravel and sand aprons that we term "zebra stripes" (Fig. 12A; Owen, 2009). The stripes are well sorted, with largest particles in the downslope position and increasingly finer particles in the upslope position (Fig. 12B). These stripes are clearly the results of overland flow events, though estimates of the rainfall intensities needed to move these sediments suggest that they must be both large and rare. Preliminary rainfall simulations of large precipitation events (~2 cm d^{-1}) seem incapable of generating overland flow (Owen, 2009). Additional features indicating unusual water availability are pipes and "spouts" visible on certain sloping landscapes. Near Aguas Blancas, on the escarpment between two river terraces, small spouts are visible (Fig. 12C), and there are

numerous pipes that run subhorizontally below the land surface (Fig. 12D). The pipes, which have formed through the dissolution sulfate, are sometimes lined discontinuously with carbonate. These indicate the presence of water having a relatively low sulfate activity (e.g., dilute). This appears to be the only chemistry that allows carbonate to form in this low pCO_2 soil environment (Ewing et al., 2006; Quade et al., 2007). Once again, the magnitude of water needed to infiltrate, and then flow downslope and produce pipes and "spouts," seems to exceed any historic rainfall events. Finally, an even more indicative feature is the frequent occurrence of rills—often co-occurring with the stripes. So we see evidence of shallow dissection and surface organization of stones, but not enough to cause deep incision or cause debris flows.

In sum, while the totality of the Atacama landscape can only be produced, and maintained, by extreme and long-term hyperaridity, there are smaller details embedded in the landscape indicating modest, and possibly rare, fluvial activity. Given the present climate conditions, it is possible that these are relict Pleistocene features. Nonetheless, the duration of these hydrological events has been insufficient to strip the landscape of its hyperarid blanket of soil and salt.

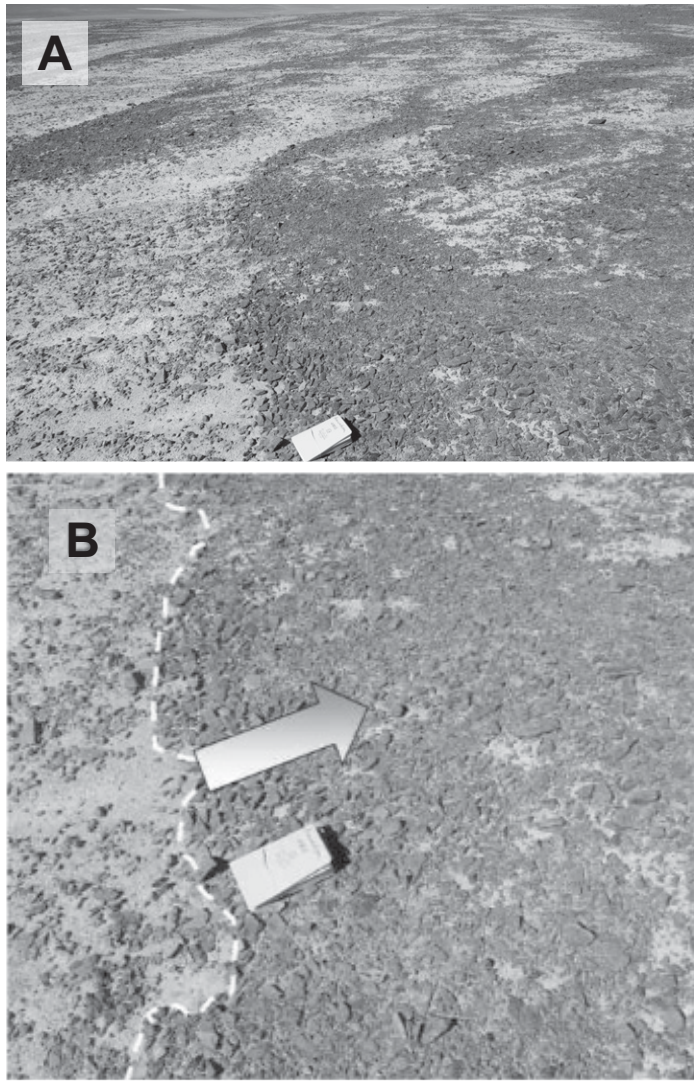

Figure 12 (*on this and following page*). Photographs showing evidence of Quaternary precipitation events or cycles exceeding the present-day norm. (A) Photograph of "zebra stripes" on hillslope near Aguas Blancas. (B) Close-up of A, showing distinctive particle sorting of the gravelly "stripe" (coarser particles in downslope direction) with a distinctive "lip" eroded immediately downslope of the coarsest particles. The arrow is pointing upslope. The object in sections A and B is a 12 × 19 cm notebook.

Correspondence of Atacama Geomorphic and Pedological Record to Global Climate

Ravelo et al. (2004) and Wara et al. (2005) examined high- to low-latitude marine sediment records for the Pliocene to the present to determine the regional marine responses to the general global cooling occurring during this period. The records recording high-latitude climate ($\delta^{18}O$ values of benthic foraminifera) indicate that an early Pliocene warm period, with temperature ~3 °C warmer than today, was terminated by an onset of Northern Hemisphere glaciation, and the development of obliquity-related cycles in the $\delta^{18}O$ values ("41 k.y. world") at ca. 2.75 Ma.

Tropical and subtropical regions, however, showed a prolonged two-phase set of changes in climate. In addition to the effects of Northern Hemisphere glaciation, Ravelo et al. (2004) proposed that a "tropical/subtropical reorganization" occurred between 1.5 and 2.0 Ma based on records of African monsoon, West African margin sea-surface temperature, and California margin biogenic carbonate deposition rates. They proposed that the climate change observed at the Northern Hemisphere glaciation transition occurred when subtropical conditions were stable and El Niño–like. Based on evidence in marine records, the authors suggest that at ca. 2.0 Ma, the tropics and subtropics switched into the modern mode of strong Walker circulation and cool subtropical sea-surface temperatures. Thus, there was an asynchronicity of climate change between high and low latitudes, with low-latitude change occurring late in the Pliocene. The authors further suggested that the development of cooler surface conditions near the tropics was achieved by changes in the ocean's thermocline (upwelling) and in the ocean's temperature gradient. In support of this hypothesis, Wara et al. (2005) further examined the east-west Pacific sea-surface temperature gradients from the Pliocene to the present based on the $\delta^{18}O$ values of surface dwelling foraminifera. The data indicate that beginning at ca. 2.3 Ma, the temperature difference between the eastern and western Pacific steadily increased, and by ca. 1.7 Ma, it was approaching present, La Niña–like, conditions.

A "permanent Pliocene El Niño" in the southern Pacific would have induced significant changes in precipitation patterns (Ravelo et al., 2006). Briefly, the reduced E-W sea-surface temperature gradients that occur during our present El Niños shift the focal point of subsiding dry air further to the east over South America (Molnar and Cane, 2002). Coincident with this, the rising moist air in the western Pacific moves to the east, reducing precipitation

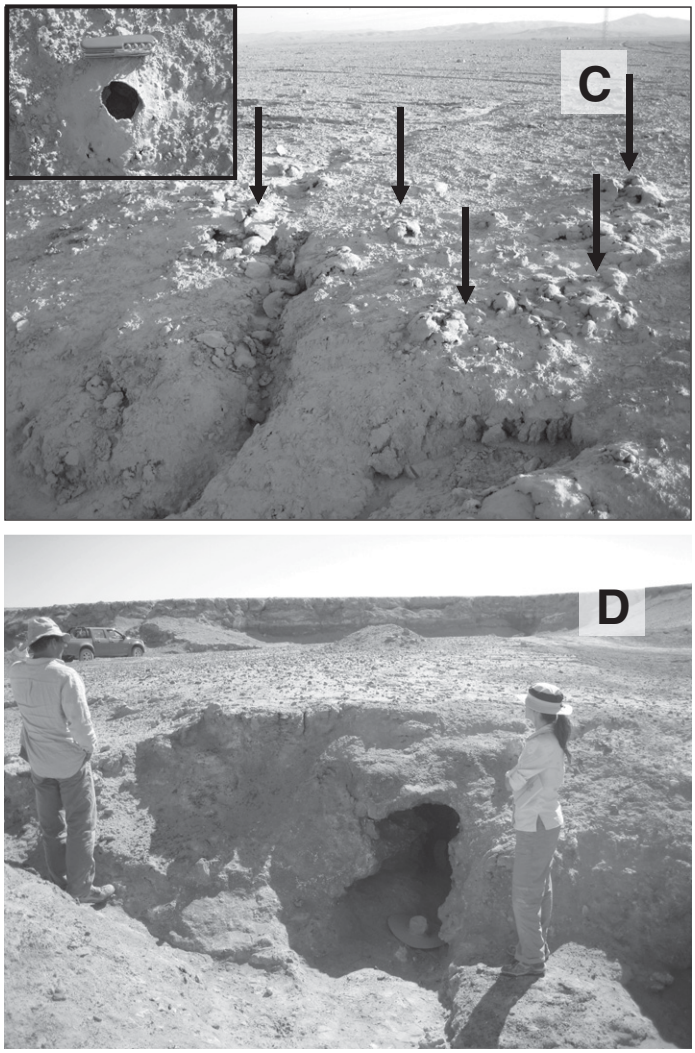

Figure 12 (*continued*). (C) A small fault scarp near La Negra showing an array of "spouts" of pipes that run parallel to the land surface a few tens of centimeters below the soil. Inset shows a "spout" in close-up. Spouts are the termination of long pipes that run through relatively porous gypsum layers that overlie more dense gypsum. Pipes are commonly coated with calcium carbonate, indicative of relatively dilute waters and low sulfate activities. (D) Large pipes in sulfate-rich soil downslope of a waterfall formed by coalescing spouts and channels.

in the western Pacific and increasing it in the eastern Pacific. The impact of oceanic cooling on Atacama climate was recently considered, along with Andean uplift, in a modeling effort by Garreaud et al. (2010). Those authors found that Andean uplift did not appear to be responsible for the onset of hyperaridity, whereas cooling of the southeast tropical Pacific at ca. 3 Ma would result in declines in precipitation, consistent with our observations and those of Hartley and Chong (2002). The impact of the modern El Niño on the precipitation of the Atacama Desert is still being evaluated: Houston (2006) provided a detailed summary. In the present winter rainfall zone (all our field areas), winter rainfall is higher in El Niño years. This trend increases with increasing latitude (Houston, 2006). There is also a correlation between strong El Niño events and catastrophic flooding in Antofagasta (Garreaud and Rutllant, 1996).

If the change from a Pliocene "permanent El Niño" to the ENSO climate system were responsible for the aridification of the Atacama Desert, there should be contemporaneous changes noted in terrestrial and marine records, within the same latitudinal belt in other parts of the world. Recently, Dupont et al. (2005) examined a high-resolution pollen record of sediments in the southeastern Atlantic, recording the vegetational history of Namibia, the African equivalent of the Atacama Desert. These authors noted that a general decline in grass pollen occurred during the Pliocene, with greatly increased variability (grass [warm] vs. semiarid [cool]) after 2.7 Ma. Van der Wateren and Dunai (2001) observed the onset of canyon incision in the Namib Desert at about this time. These observations are consistent with a general increase in pole-equatorial temperature gradients, decreased low-latitude precipitation, increased Hadley circulation, and strengthening of trade winds. In addition to these changes, the pollen record also suggests a northward shift in westerly frontal systems and winter rainfall between 3.1 and 2.2 Ma. At 2.2 Ma, the pollen influx for the Namibia region greatly declined, with a corresponding drop in Cyperacease pollen (plants growing along rivers and marshes; Dupont et al., 2005). The decline in the marsh-loving plants is interpreted as a drop, or cessation, of riverine sediments from Namibia. The authors propose that the climate change may have been due to a switch of the central Namibian upwelling system from one of predominately advection of subpolar water to increased upwelling, resulting in a decline in sea-surface temperatures (and precipitation). As the authors noted, this onset of aridification occurred slightly earlier than the 1.7–2.0 Ma increase in El Niño–Southern Oscillation variability proposed by Ravelo et al. (2004).

In Australia, which has a strong El Niño/La Niña response to rainfall, one would expect that a permanent El Niño would have created drier conditions than those of today. Yet, as Molnar and Cane (2002) have noted, paleontological evidence suggests that the reverse may have been true. In addition, recent cosmogenic nuclide dating of the formation of desert pavements (gibbers) indicates that they underwent a significant formation phase ca. 4–2 Ma, as the region became drier (rather than wetter; Fujioka et al. 2005). This, interpretation is consistent with previous Australian records but exists as a somewhat unique exception to trends in this latitudinal belt (Molnar and Cane, 2002).

The timing of both Pacific surface temperatures and the vegetation change in sediments offshore of Namibia are remarkably consistent with the timing of apparent hyperaridification of the Atacama Desert. The timing of the geomorphic events is less precise, and constrains only the terminal stages of the geomorphic response, not the onset. Nevertheless, our results are consistent with the recent work of Hartley and Chong (2002). These authors observed that in the Central Depression (~22.5°S), lacustrine and fluvial sedimentation was nearly continuous from early Miocene to late Pliocene times, when deposition ceased at ca. 3 Ma. Except for a distinct anhydrite horizon indicating hyperaridity at 6 Ma, the sedimentary record indicates that semiarid conditions prevailed until the late Pliocene.

These authors attribute the aridification to global climate change rather than the strength of the Humboldt Current or Andean uplift. However, as argued by Ravelo et al. (2004) and Dupont et al. (2005), these may not be entirely independent, and globally driven climate change can enhance or change the magnitude of coastal upwelling, and drive subtropical climate change.

Comparison to Other Constraints on Hyperaridity in the Atacama Desert

Here, we briefly examine previously published studies on the onset of hyperaridity in the Atacama Desert. These studies include: (1) Oligocene–Miocene ^{21}Ne exposure ages in surface boulders on a terrace remnant along the Quebrada de Tiliviche at 19.30°S (Dunai et al., 2005), (2) Miocene ages of the cessation of supergene Cu enrichment near La Escondida (Alpers and Brimhall, 1988), (3) nitrate and sulfate Miocene paleosols in the vicinity of Calama (Rech et al., 2006), and (4) cosmogenic radionuclide exposure ages from numerous surface samples (Placzek et al., 2010).

Dunai et al. (2005) examined an alluvial-fan remnant found in a faulted segment of the Coastal Cordillera near Pisagua, Chile. The ^{21}Ne exposure ages ranged from ca. 4 to 37 Ma, ages spanning the Pliocene to Oligocene-Eocene boundary. The presence of the Oligocene-aged cobbles was interpreted as suggesting that the surface had been preserved since that time, and that this signaled a prolonged hyperarid condition. The broad range in exposure ages casts uncertainty on the true age of the surface, and by association its climatic significance. This location has also been examined in detail by Allmendinger et al. (2005). The Pisagua fault scarp is located immediately south of the sample locations of Dunai et al. (2005). Allmendinger et al. (2005) dated a fluvially deposited volcanic ash embedded in fault folded sediments, arriving at an age of 3.49 ± 0.04 Ma, indicating that local fluvial activity was active in the Pliocene. Additionally, the region immediately to the east is dominated by a thick, sedimentary infill that terminated in the Miocene, based on extension to the well-dated landscapes north of 19.0°S (García et al., 2004). Due either to uplift or coastal retreat (Allmendinger et al., 2005), river channels draining the Andes have subsequently carved deep canyons into this Miocene sediment. Local drainages (post-Miocene) have been unable to adjust to modest faulting on the alluvial fans, resulting in several episodes of stream diversion. In summary, while it is clear that more extensive landform dating in this area is needed to fully reconstruct the fluvial history, the presence of large Miocene fluvial deposits and modest to minor post-Miocene or Pliocene modification of these surfaces by drainages confined to the Central Depression suggest either multiple periods of hyperaridity, or (we argue) its relatively late-stage onset.

One of the most widely cited constraints on the onset of hyperaridity in the Atacama Desert is the work of Alpers and Brimhall (1988), who reported K/Ar ages on supergene minerals at La Escondida that range from 14.7 to 18 Ma. At this and other supergene deposits, the cessation of supergene enrichment of porphyry Cu deposits is interpreted to represent a significant decline in water infiltration and weathering. However, as Hartley and Rice (2005) reported, as the number of ages generated from supergene Cu deposits in Chile increases, the radiometric age range has also increased. Data compiled by Hartley and Rice (2005) show that supergene ages range from 6 to 44 Ma. Most recently, Reich et al. (2009) have further extended this analysis. They noted that oxide- and hydroxide-rich supergene ores (requiring meteoric waters) declined after 9 Ma, and ceased at 5 Ma. Since then, U-series dating of sulfates suggests that the most recent phase of Cu enrichment was due to the formation of atacamite from saline groundwaters. These authors noted that this apparent sequence of Cu ore enrichment is consistent with Hartley and Chong's (2002) suggestion of Pliocene aridification.

The presence of sulfate and nitrate in Miocene paleosols of the Calama basin has been recently reported, and it has been interpreted to indicate a Miocene period of hyperaridity (Rech et al., 2006). These paleosols appear (based on regional geological mapping and field observations) to represent fan facies that graded into a large regional salar/lacustrine system, and thus were adjacent to a significant regional salt source accumulated by stream systems trapped in a large internal basin behind the Coastal Ranges (Sáez et al., 1999). Even with the large salt source, the presence of these well-developed aridic paleosols is clearly indicative of hyperarid conditions. The length that this period of aridity persisted is unknown since a longer record of paleosols has not yet been identified in the region.

Most recently, Placzek et al. (2010) reported on ^{10}Be, ^{26}Al, and ^{21}Ne exposure ages and/or erosion rates for a variety of surficial samples along a W-E transect at the approximate latitude of Antofagasta. Apparent exposure ages were lower (and erosion rates higher) in both the coastal and pre-Andean ranges. Factors of interest here include: (1) The oldest exposure ages were ca. 2–2.5 Ma, and (2) there was a cluster of other samples with exposure ages of ca. 1 Ma. There are some difficulties interpreting these results directly in relation to the focus of this paper. First, the locations and mapped geomorphic/geological units from which the samples were obtained were not presented by Placzek et al. (2010), so the relationship between exposure age and mapped landform is not clear. Second, we (Table 2) found numerous surficial samples in the same region for which ^{10}Be exposure ages exceeded 2 Ma (with a maximum of 6.4 Ma), ages that match the mapped geological units (see GSA Data Repository figures [see footnote 2]). These older ages are also matched by published K-Ar ages of ash embedded in sediment (Table 2). One interpretation to reconcile these differences would be that Placzek et al. (2010) collected samples (at least those from alluvial deposits) that coincide with two out of the three major geomorphic units in the region (the Quaternary and Pliocene, but not the Miocene deposits). However, as those authors noted, and as we discussed earlier, the entire region bears the telltale marks of periodic pulses of moisture that appear to exceed historical observations, and thus finding surficial gravels for which cosmogenic nuclide concentrations truly represent or approach the age of the deposit itself requires considerable field work and rigorous sampling criteria.

The Atacama Desert contains considerable thicknesses of basin fills that have been exposed via stream incision or through the drilling (Hartley and Chong, 2002). While these basin sediments are impacted by tectonics as well as climate, the chemical changes in basin sediments were interpreted by Hartley and Chong (2002) to suggest that semiarid conditions persisted throughout most of the Miocene, and that the onset of continuous hyperaridity occurred in the Pliocene.

To summarize, the presence of Miocene–Pliocene (and possibly older) salar deposits and well-preserved fluvial surfaces is a striking feature of the Atacama Desert, one that suggests a long-term period of low rainfall. However, the fact that the Atacama Desert bears distinct regional fluvial features of post-Miocene age indicates that hyperaridity has not been constant over this long time span.

CONCLUSIONS

The fluvial and pedogenic features in the Atacama Desert record information on the origin and persistence of hyperaridity. Stream incision and erosion were reduced to almost insignificant levels following the late Pliocene to the early Pleistocene. Hillslopes appear to have shed their silicate soil mantle and were stripped to hard bedrock at the end of the Pliocene. Since then, these hillslopes have been draped in dust and salt, exceedingly mobile particles that have nonetheless persisted over the course of the

Quaternary. While the region is not fluvially or pedogenically dead, nor exempt from smaller-scale climate oscillations, the rates of processes are now so slow (on an average rate) that the time frame required to detect observable change is orders of magnitude greater than most places on Earth. Thus, the unusual features on the landscapes, such as striping of gravels on hillslopes, suggest the importance of rare or unique rainfall events, or the persistence of such features as relicts from past somewhat moister climates. However, the magnitude of climate shifts must have remained small to maintain the large quantities of soil salts. Most significantly, many of the general topographic features (mountain ranges, canyons, convex hillslopes) appear to be relicts from a pre-Miocene landscape that have persisted to the present time.

The occurrence of vast areas of fluvial deposits just older than 2 Ma, and the presence of alluvial fans surrounding hillslopes of the same age, suggests a major climate change that greatly changed the fluvial capacity of the stream systems. The near-contemporary changes in geomorphology and paleontology that occurred in the Namibian desert, and the similarity of timing of changes in both deserts to changes in sea-surface temperatures and the onset of the present ENSO circulation system suggest that both regions responded to a global climatic change, one that now characterizes our present world.

The importance of the ENSO system to the hyperaridity of the Atacama Desert raises interesting questions regarding the impact of anthropogenic global warming on the South Pacific climate system. Reports of the weakening of the tropical Pacific circulation during the past century, a trend attributed to anthropogenic forcing (Vecchi et al., 2006), may reduce the strength of normal climate patterns and increase "El Niño–like" conditions, though this possibility is still highly uncertain (Collins et al., 2005). However, recent regional climate modeling of the tropical Andes, under several late twenty-first century emission scenarios, suggests that the hyperarid coast of Peru and northern Chile may receive up to 100% more rainfall than today (between 0 and 400 mm absolute increase; Urrutia and Vuille, 2009). In modern Chile, regions to the south of the desert that receive only a few millimeters more precipitation than the hyperarid heart of the Atacama are stripped of salts and dust to bedrock. Thus, if the Pacific climate system undergoes even a small measurable change, more than 2 m.y. worth of salts and dust are poised to be readily mobilized by small increases in moisture, raising the troubling question as to the long-term future of one of the most unique biomes on the planet.

ACKNOWLEDGMENTS

Funding for this research was provided by a National Science Foundation Geobiology and Low Temperature Geochemistry grant to Amundson and Nishiizumi. A National Aeronautics and Space Administration graduate fellowship supported Owen and Ewing.

REFERENCES CITED

Allmendinger, R.W., González, G., Yu, J., Hoke, G., and Isacks, B., 2005, Trench parallel shortening in the northern Chilean forearc: Tectonic and climatic implications: Geological Society of America Bulletin, v. 117, p. 89–104, doi:10.1130/B25505.1.

Alpers, C.N., and Brimhall, G.H., 1988, Middle Miocene climatic change in the Atacama Desert, northern Chile: Evidence from supergene mineralization at La Escondida: Geological Society of America Bulletin, v. 100, p. 1640–1656, doi:10.1130/0016-7606(1988)100<1640:MMCCIT>2.3.CO;2.

Basso, M., 2004, Carta Baquedono, Region de Antofagasta, Carta Geologica de Chile, Serie Geologoa Basica, No. 82.

Betancourt, J.L., Latorre, C., Rech, J.A., Quade, J., and Rylander, K.A., 2000, A 22,000-year record of monsoonal precipitation from northern Chile's Atacama Desert: Science, v. 289, p. 1542–1546, doi:10.1126/science.289.5484.1542.

Bookhagen, B., and Strecker, M.R., 2008, Orographic barriers, high-resolution TRMM rainfall, and relief variations along the eastern Andes: Geophysical Research Letters, v. 35, doi:10.1029/2007GL032011.

Clark, A.H., Myers, A.E.S., Mortimer, C., Sillitoe, R.H., Cook, R.V., and Snelling, N.J., 1967, Implications of the isotopic ages of ignimbrite flows, southern Atacama Desert, Chile: Nature, v. 215, p. 723–724, doi:10.1038/215723a0.

Collins, R.E., and the CMIP Modelling Groups, 2005, El Niño– or La Niña–like climate change?: Climate Dynamics, v. 24, p. 89–104, doi:10.1007/s00382-004-0478-x.

Cortés, J.A., 2000, Hoja Palestina. Region de Antofagasta: SERNAGEOMIN (Chile) Mapas Geologicos 19, scale 1:100,000.

Darwin, C., 1845, Journal of Researches into the Natural History and Geology of the Countries Visited during the Voyage of the *H.M.S. Beagle* Round the World, under the Command of Capt. Fitz Roy, R.N., 2nd Ed.: London, John Murray, 536 p.

Dietrich, W.E., Reiss, R., Hsu, M.L., and Montgomery, D.R., 1995, A process-based model for colluvial soil depth and shallow landsliding using digital elevation data: Hydrological Processes, v. 9, p. 383–400, doi:10.1002/hyp.3360090311.

Dunai, T.J., González López, G.A., and Juez-Larré, J., 2005, Oligocene–Miocene age of aridity in the Atacama Desert revealed by dating of erosion-sensitive landforms: Geology, v. 33, p. 321–324, doi:10.1130/G21184.1.

Dupont, L.M., Donner, B., Vidal, L., Pérez, E.L., and Wefer, G., 2005, Linking desert evolution and coastal upwelling: Pliocene climate change in Namibia: Geology, v. 33, p. 461–464, doi:10.1130/G21401.1.

Ericksen, G.E., 1981, Geology and Origin of the Chilean Nitrate Deposits: U.S. Geological Survey Professional Paper 1188, 37 p.

Ewing, S.A., Sutter, B., Owen, J., Nishiizumi, K., Sharp, W., Cliff, S.S., Perry, K., Dietrich, W., McKay, C.P., and Amundson, R., 2006, A threshold in soil formation at Earth's arid-hyperarid transition: Geochimica et Cosmochimica Acta, v. 70, p. 5293–5322, doi:10.1016/j.gca.2006.08.020.

Ewing, S.A., Michalski, G., Thiemens, M., Quinn, R.C., Macalady, J.L., Kohl, S., Wankel, S.D., Kendall, C., McKay, C.P., and Amundson, R., 2007, Rainfall limit of the N cycle on Earth: Global Biogeochemical Cycles, v. 21, GB3009, doi:10.1029/2006GB002838.

Ewing, S.A., Macalady, J.L., Warren-Rhodes, K., McKay, C.P., and Amundson, R., 2008a, Changes in the soil C cycle at the arid-hyperarid transition in the Atacama Desert: Journal of Geophysical Research, v. 113, G02S90, doi:10.1029/2007JG000495.

Ewing, S.A., Yang, W., DePaolo, D.J., Michalski, G., Kendall, C., Stewart, B.W., Thiemens, M., and Amundson, R., 2008b, Non-biological fractionation of stable Ca isotopes in soils of the Atacama Desert, Chile: Geochimica et Cosmochimica Acta, v. 72, p. 1096–1110, doi:10.1016/j.gca.2007.10.029.

Fujioka, T., Chappell, J., Honda, M., Yatsevich, I., Fifield K., and Fabel, D., 2005, Global cooling initiated stony deserts in central Australia 2-4 Ma, dated by cosmogenic ^{21}Ne-^{10}Be. Geology, v. 33, p. 993–996.

García, M., Gardeweg, M., Clavero, J., and Hérail, G., 2004, Hoja Arica: Servicio Nacional de Geología y Minería (Chile) Carta Geologica de Chile 84.

Garreaud, R.D., and Rutllant, J., 1996, Análisis meteorológico de los aluviones de Antofagasta y Santiago de Chile en el período 1991–1993: Atmósfera, v. 9, p. 251–271, scale 1:250,000.

Garreaud, R.D., Molina, A., and Farias, M., 2010, Andean uplift, ocean cooling and Atacama hyperaridity: A climate modeling perspective: Earth and Planetary Science Letters, v. 292, p. 39–50, doi:10.1016/j.epsl.2010.01.017.

Gibbard, P.L., Head, M.J., and Walker, M.J.C., and The Subcommission on Quaternary Stratigraphy, 2009, Formal ratification of the Quaternary System/Period and the Pliestocene Series/Epoch with a base at 2.58 Ma: Journal of Quaternary Science, v. 25, p. 96-102.

González, G., and Niemeyer, H., 2005, Cartas Antofagasta y Punta Tetas. Región de Antofagasta: Servicio Nacional de Geologia y Mineria (Chile) Carta Geologica de Chile, Serie Geologia Basica 89, scale 1:100,000.

González, G.L., Dunai, T., Carrizo, D., and Allmendinger, R., 2006, Young displacements on the Atacama fault system, northern Chile, from field observation and cosmogenic ^{21}Ne concentrations: Tectonics, v. 25, TC3006, doi:10.1029/2005TC001846.

Hartley, A.J., and Chong, G., 2002, Late Pliocene age for the Atacama Desert: Implications for the desertification of western South America: Geology, v. 30, p. 43–46, doi:10.1130/0091-7613(2002)030<0043:LPAFTA>2.0.CO;2.

Hartley, A.J., and Rice, C.M., 2005, Controls on supergene enrichment of porphyry copper in the Central Andes: A review and discussion: Mineralium Deposita, v. 40, p. 515–525, doi:10.1007/s00126-005-0017-7.

Hebbeln, D., Lamy, F., Mohtadi, M., and Echtler, H., 2007, Tracing the impact of glacial-interglacial climate variability on erosion of the southern Andes: Geology, v. 35, p. 131–134, doi:10.1130/G23243A.1.

Heimsath, A.M., Dietrich, W.E., Nishiizumi, K., and Finkel, R.C., 1999, Cosmogenic nuclides, topography, and the spatial variation of soil depth: Geomorphology, v. 27, p. 151–172, doi:10.1016/S0169-555X(98)00095-6.

Heimsath, A.M., Chappell, J., Dietrich, W.E., Nishiizumi, K., and Finkel, R.C., 2001, Late Quaternary erosion in southeastern Australia: Quaternary International, v. 83–85, p. 169–185, doi:10.1016/S1040-6182(01)00038-6.

Houston, J., 2006, Variability of precipitation in the Atacama Desert: Its causes and hydrological impact: International Journal of Climatology, v. 26, p. 2181–2198, doi:10.1002/joc.1359.

Hutchinson, M.F., 1989, A new procedure for gridding elevation and stream line data with automatic removal of spurious pits: Journal of Hydrology (Amsterdam), v. 106, p. 211–232, doi:10.1016/0022-1694(89)90073-5.

Hutchinson, M.F., 1996, A locally adaptive approach to the interpolation of digital elevation models, *in* Proceedings of the Third International Conference/Workshop on Integrating GIS and Environmental Modeling (Santa Fe, New Mexico, 21–26 January 1996): Santa Barbara, California, National Center for Geographic Information and Analysis, http://www.ncgia.ucsb.edu/conf/SANTA_FE_CD-ROM/main.html.

Jordan, T.E., Nester, P.L., Blanco, N., Hoke, G.D., Davila, F., and Tomlinson, A.J., 2010, Uplift of the Altiplano-Puna Plateau: A view from the west: Tectonics, v. 29, doi:10/1029/2010TC002661.

Kohl, C.P., and Nishiizumi, K., 1992, Chemical isolation of quartz for measurement of in-situ–produced cosmogenic nuclides: Geochimica et Cosmochimica Acta, v. 56, p. 3583–3587, doi:10.1016/0016-7037(92)90401-4.

Lal, D., 1991, Cosmic ray labeling of erosion surfaces: In situ nuclide production rates and erosion models: Earth and Planetary Science Letters, v. 104, p. 424–439, doi:10.1016/0012-821X(91)90220-C.

Lamb, S., and Davis, P., 2003, Cenozoic climate change as a possible cause for the rise of the Andes: Nature, v. 425, p. 792–797, doi:10.1038/nature02049.

Lamb, S., and Hoke, L., 1997, Origin of the high plateau in the Central Andes, Bolivia, South America: Tectonics, v. 16, p. 623–649, doi:10.1029/97TC00495.

Leonard, E.M., and Wehmiller, J.F., 1992, Low uplift rates and terrace reoccupation inferred from mollusk aminostratigraphy, Coquimbo Bay Area, Chile: Quaternary Research, v. 38, p. 246–259, doi:10.1016/0033-5894(92)90060-V.

Le Roux, J.P., Gómez, C., Venegas, C., Fenner, J., Middleton, H., Marchant, M., Buchbinder, B., Frassinetti, D., Marquardt, C., Gregory-Wodzicki, K.M., and Lavenu, A., 2005, Neogene–Quaternary coastal and offshore sedimentation in north central Chile: Record of sea-level changes and implications for Andean tectonism: Journal of South American Earth Sciences, v. 19, p. 83–98, doi:10.1016/j.jsames.2003.11.003.

Maier, R.M., Drees, K.P., Neilson, J.W., Henderson, D.A., Quade, J., and Betancourt, J.L., 2004, Microbial life in the Atacama Desert: Science, v. 306, 1289c, doi:10.1126/science.306.5700.1289c.

Marinovic, N., and García, M., 1999, Hoja Pampa Union. Region de Antofagasta: Servicio Nacional de Geologia y Mineria (Chile) Mapas Geologicos 9, scale 1:100,000.

Marinovic, N., Smoje, I., Maksaev, V., Herve, M., and Mpodozis, C., 1992, Hoja Aguas Blancas: Servicio Nacional de Geologia y Mineria (Chile) Carta Geologica de Chile 70, scale 1:250,000.

Marquardt, C., Lavenu, A., Ortlieb, L., Godoy, E., and Comte, D., 2004, Coastal neotectonics in southern Central Andes: Uplift and deformation of marine terraces in northern Chile (27°S): Tectonophysics, v. 394, p. 193–219, doi:10.1016/j.tecto.2004.07.059.

Mayer, L., McFadden, L.D., and Harden, J.W., 1988, Distribution of calcium carbonate in desert soils: A model: Geology, v. 16, p. 303–306, doi:10.1130/0091-7613(1988)016<0303:DOCCID>2.3.CO;2.

McFadden, L.D., Wells, S.G., and Jercinovich, M.J., 1987, Influences of eolian and pedogenic processes on origin and evolution of desert pavements: Geology, v. 15, p. 504–508, doi:10.1130/0091-7613(1987)15<504:IOEAPP>2.0.CO;2.

Michalski, G., Bohlke, J.K., and Thiemens, M., 2004, Long term atmospheric deposition as the source of nitrate and other salts in the Atacama Desert, Chile: New evidence from mass-independent oxygen isotope compositions: Geochimica et Cosmochimica Acta, v. 68, p. 4023–4038, doi:10.1016/j.gca.2004.04.009.

Molnar, P., and Cane, M.A., 2002, El Niño's tropical climate and teleconnections as a blueprint for pre–Ice Age climates: Paleoceanography, v. 17, doi:10.1029/2001PA000663.

Montgomery, D.R., Balco, G., and Willett, S.D., 2001, Climate, tectonics, and the morphology of the Andes: Geology, v. 29, p. 579–582, doi:10.1130/0091-7613(2001)029<0579:CTATMO>2.0.CO;2.

Mortimer, C., 1973, The Cenozoic history of the southern Atacama Desert, Chile: Journal of the Geological Society of London, v. 129, p. 505–526, doi:10.1144/gsjgs.129.5.0505.

Mortimer, C., 1980, Drainage evolution in the Atacama Desert of northernmost Chile: Revista Geológica de Chile, v. 11, p. 3–28.

Nalpas, T., Dabard, M.-P., Ruffet, G., Vernon, A., Mpodozis, C., Loi, A., and Hérail, G., 2008, Sedimentation and preservation of the Miocene Atacama Gravels in the Pedernales-Chañaral area, northern Chile: Climatic or tectonic control?: Tectonophysics, v. 459, p. 161–173, doi:10.1016/j.tecto.2007.10.013.

Naranjo, J.A., and Puig, A., 1984, Taltal y Chañaral. Servicio Nacional de Geología y Minería, Carta Geológica de Chile, Nos. 62-63 (escala 1:250,000).

Navarro-González, R., Rainey, F.A., Molina, P., Bagaley, D.R., Hollen, B.J., de la Rosa, J., Small, A.M., Quinn, R.C., Grunthaner, F.J., Cáceres, L., Gomez-Silva, B., and McKay, C.P., 2003, Mars-like soils in the Atacama Desert, Chile, and the dry limit of microbial life: Science, v. 302, p. 1018–1021, doi:10.1126/science.1089143.

Nishiizumi, K., 2003, Preparation of ^{26}Al AMS standards: Nuclear Instruments and Methods in Physics Research, v. 223–224, p. 388–392.

Nishiizumi, K., Imamura, M., Caffee, M., Southon, J.R., Finkel, R.D., and McAninch, J., 2007, Absolute calibration of ^{10}Be AMS standards: Nuclear Instruments and Methods in Physics Research, v. 258, p. 403–413, doi:10.1016/j.nimb.2007.01.297.

Ortlieb, L., Zazo, C., Goy, J.L., Hillaire-Marcel, C., Ghaleb, B., and Cournoyer, L., 1996, Coastal deformation and sea-level changes in the northern Chile subduction area (23°S) during the last 330 ky: Quaternary Science Reviews, v. 15, p. 819–831, doi:10.1016/S0277-3791(96)00066-2.

Ota, Y., Miyauchi, T., Paskoff, R., and Koba, M., 1995, Plio–Quaternary terraces and their deformation along the Altos de Talinay, north-central Chile: Revista Geológica de Chile, v. 22, p. 89–102.

Owen, J.J., 2009, Soil formation and geomorphology along a precipitation gradient in the Atacama Desert, Chile [Ph.D. dissertation]: Berkeley, California, University of California, 174 p.

Owen, J.J., Amundson, R., Dietrich, W.E., Nishiizumi, K., Sutter, B., and Chong, G., 2010, The sensitivity of hillslope bedrock erosion to precipitation: Earth Surface Processes and Landforms, v. 36, p. 117–135, doi:10.1002/esp.2083.

Placzek, C.J., Matmon, A., Granger, D.E., Quade, J., and Niedermann, S., 2010, Evidence for active landscape evolution in the hyperarid Atacama from multiple terrestrial cosmogenic nuclides: Earth and Planetary Science Letters, v. 295, p. 12–20, doi:10.1016/j.epsl.2010.03.006.

Quade, J., Rech, J.A., Latorre, C., Betancourt, J.L., Gleeson, E., and Kalin, M.T.K., 2007, Soils at the hyperarid margin: The isotopic composition of soil carbonate from the Atacama Desert: Northern Chile: Geochimica et Cosmochimica Acta, v. 71, p. 3772–3795, doi:10.1016/j.gca.2007.02.016.

Quezada, J., Gonzalez, G., Dunai, T., Jensen, A., and Juez-Larre, J., 2007, Pleistocene littoral uplift of northern Chile: Ne-21 age of the upper marine terrace of Caldera-Bahia Inglesa area: Revista Geológica de Chile, v. 34, p. 81–96.

Ravelo, A.C., Andreasen, D.H., Lyle, M., Lyle, A.O., and Wara, M.W., 2004, Regional climate shifts caused by gradual global cooling in the Pliocene epoch: Nature, v. 429, p. 263–267, doi:10.1038/nature02567.

Ravelo, A.C., Dekens, P.S., and McCarthy, M., 2006, Evidence for El Niño–like conditions during the Pliocene: GSA Today, v. 16, no. 3, p. 4–11, doi:10.1130/1052-5173(2006)016<4:EFENLC>2.0.CO;2.

Rech, J., Quade, J., and Hart, W.S., 2003, Isotopic evidence for the source of Ca and S in soil gypsum, anhydrite, and calcite in the Atacama Desert: Geochimica et Cosmochimica Acta, v. 67, p. 575–586, doi:10.1016/S0016-7037(02)01175-4.

Rech, J.A., Currie, B.S., Michalski, G., and Cowan, A.M., 2006, Neogene climate change and uplift in the Atacama Desert, Chile: Geology, v. 34, p. 761–764, doi:10.1130/G22444.1.

Rehak, K., Bookhagen, B., Strecker, M.R., and Echtler, H.P., 2010, The topographic imprint of a transient climate episode: The western Andean flank between 15.5° and 41.5°S: Earth Surface Processes and Landforms, v. 35, p. 1516–1534, doi:10.1002/esp.1992.

Reich, M., Palacios, C., Vargas, G., Luo, S., Cameron, E.M., Leybourne, M.I., Parada, M.A., Zuniga, A., and You, C.-F., 2009, Supergene enrichment of copper deposits since the onset of modern hyperaridity in the Atacama Desert, Chile: Mineralium Deposita, v. 44, p. 497–504, doi:10.1007/s00126-009-0229-3.

Riquelme, R., Hérail, G., Martinod, J., Charrier, R., and Darrozes, J., 2007, Late Cenozoic geomorphic signal of Andean forearc deformation and tilting associated with the uplift and climate change of the southern Atacama Desert (26°S–28°S): Geomorphology, v. 86, p. 283–306, doi:10.1016/j.geomorph.2006.09.004.

Rutllant, J.A., Fuenzalida, H., and Aceituno, P., 2003, Climate dynamics along the arid northern coast of Chile: The 1997–1998 Dinámica del Clima de la Región de Antofagasta (DICLIMA) experiment: Journal of Geophysical Research, v. 108, doi:10.1029/2002JD003357.

Sáez, A., Cabrera, L., Jensen, A., and Chong, G., 1999, Late Neogene lacustrine record and palaeogeography in the Quillagua-Llamara basin, Central Andean forearc (northern Chile): Palaeogeography, Palaeoclimatology, Palaeoecology, v. 151, p. 5–37, doi:10.1016/S0031-0182(99)00013-9.

Saillard, M., Audin, L., Hérail, G., Carretier, S., Regard, V., Ortlieb, L., Hall, S., Farber, D., Martinod, J., and Macharé, J., 2007, ^{10}Be and ^{26}Al dating of marine terrace to quantify the uplift of Peruvian and Chilean coastal areas: Geophysical Research Abstracts, v. 9, 05013.

Saillard, M., Hall, S.R., Audin, L., Farber, D.L., Hérail, G., Martinod, J., Regard, V., Rinkel, R.C., and Bondoux, F., 2009, Non-steady long-term uplift rates and Pleistocene marine terrace development along the Andean margin of Chile (31°S) inferred from ^{10}Be dating: Earth and Planetary Science Letters, v. 277, p. 50–63, doi:10.1016/j.epsl.2008.09.039.

Soil Survey Manual, 1993, U.S. Department of Agriculture, Natural Resources Conservation Service Soil Survey Manual: http://soils.usda.gov/technical/manual/ (last accessed March 2012).

Syvitski, J.P.M., and Milliman, J.D., 2007, Geology, geography, and humans battle for dominance over the delivery of fluvial sediment to the coastal ocean: The Journal of Geology, v. 115, p. 1–19, doi:10.1086/509246.

Urrutia, R., and Vuille, M., 2009, Climate change projections for the tropical Andes using a regional climate model: Temperature and precipitation simulations for the end of the 21st century: Journal of Geophysical Research, v. 114, doi:10.1029/2008JD011021.

Van der Wateren, F.M., and Dunai, T.J., 2001, Late Neogene passive margin denudation history—Cosmogenic isotope measurements from the central Namib Desert: Global and Planetary Change, v. 30, p. 271–307, doi:10.1016/S0921-8181(01)00104-7.

Vecchi, G.A., Soden, B.J., Witeenberg, A.T., Held, I.M., Leetma, A., and Harrison, M.J., 2006, Weakening of tropical Pacific atmospheric circulation due to anthropogenic forcing: Nature, v. 441, p. 73–76, doi:10.1038/nature04744.

von Huene, R., Weinrebe, W., and Heeren, F., 1999, Subduction erosion along the North Chile margin: Geodynamics. v. 27, p. 345–358, doi:10.1016/S0264-3707(98)00002-7.

Wahba, G., 1990, Spline models for observational data, *in* CBMS-NSF Regional Conference Series in Applied Mathematics: Philadelphia, Society for Industrial and Applied Mathematics, xii + 169 p.

Wara, M.W., Ravelo, A.C., and Delaney, M.L., 2005, Permanent El Niño–like conditions during the Pliocene Warm Period: Science, v. 309, p. 758–761, doi:10.1126/science.1112596.

Warren-Rhodes, K.A., Rhodes, K.L., Pointing, S.B., Ewing, S.A., Lacap, D.C., Gomez-Silva, B., Amundson, R., Friedman, E.I., and McKay, C.P., 2007, Hypolithic cyanobacteria, dry limit of photosynthesis, and microbial ecology in the hyperarid Atacama Desert: Microbial Ecology, v. 52, p. 389–398, doi:10.1007/s00248-006-9055-7.

Whipple, K.X., and Tucker, G.E., 1999, Dynamics of the stream-power incision model: Implications for height limits of mountain ranges, landscape response timescales, and research needs: Journal of Geophysical Research, v. 104, p. 17,661–17,674, doi:10.1029/1999JB900120.

Science Editor: Christian Koeberl
Associate Editor: Massimo Mattei

Manuscript Received 11 November 2010
Revised Manuscript Received 18 July 2011
Manuscript Accepted 16 August 2011

Printed in the USA